Hydrological control of water quality – Modelling base cation weathering and dynamics across heterogeneous boreal catchments

Elin Jutebring Sterte [a,b,*], Fredrik Lidman [a], Nicola Balbarini [c], Emma Lindborg [b], Ylva Sjöberg [d], Jan-Olof Selroos [e], Hjalmar Laudon [a]

[a] Department of Forest Ecology and Management, Swedish University of Agricultural Sciences, SE-901 83 Umeå, Sweden
[b] DHI Sweden AB, Skeppsbron 28, SE-111 30 Stockholm, Sweden
[c] DHI A/S, Agern Allé 5, 2970 Hørsholm, Denmark
[d] Center for Permafrost (CENPERM), Department of Geosciences and Natural Resource Management, University of Copenhagen, Øster Voldgade 10, 1350 Copenhagen, Denmark
[e] Svensk Kärnbränslehantering AB (SKB), Evenemangsgatan 13, 169 79 Solna, Sweden

HIGHLIGHTS

- A 3D water flow model was used to simulate base cation export and dynamics.
- 14 sub-catchments of different sizes and landscape characteristics were investigated.
- Catchment hydrology had a strong impact on the water quality.
- Weathering of K, Mg, and Ca was primarily linked to soil contact time.
- ~45% of base cation export originated from weathering of deep soils (>2.5 m).

GRAPHICAL ABSTRACT
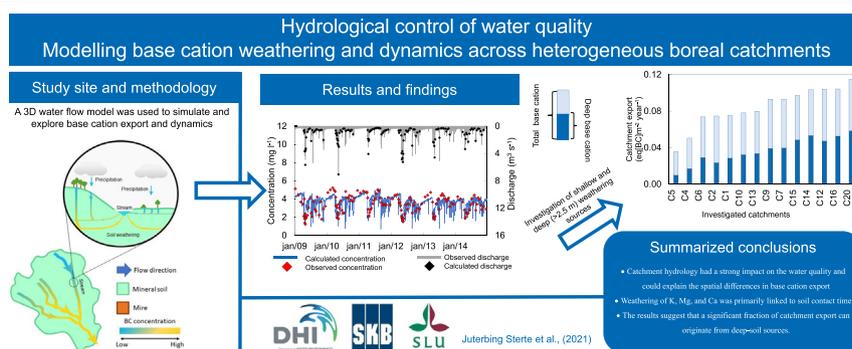
ARTICLE INFO

ABSTRACT

Linking biogeochemical processes to water flow paths and solute travel times is important for understanding internal catchment functioning and control of water quality. Base cation weathering is a process closely linked to key factors affecting catchment functioning, including water pathways, soil contact time, and catchment characteristics, particularly in silicate-dominated areas. However, common process-based weathering models are often calibrated and applied for individual soil profiles, which can cause problems when trying to extrapolate results to catchment scale and assess consequences for stream water and groundwater quality. Therefore, in this work, base cation export was instead modelled using a fully calibrated 3D hydrological model (Mike SHE) of a boreal catchment, which was expanded by adding a relatively simple but still reasonably flexible and versatile weathering module including the base cations Na, K, Mg, and Ca. The results were evaluated using a comprehensive dataset of water chemistry from groundwater and stream water in 14 nested sub-catchments, representing different catchment sizes and catchment characteristics. The strongest correlations with annual and seasonal observations were found for Ca ($r = 0.89$-0.93, $p < 0.05$), Mg ($r = 0.90$-0.95, p < 0.05), and Na ($r = 0.80$-0.89, p < 0.05). These strong correlations suggest that catchment hydrology and landscape properties primarily control weathering rates and stream dynamics of these solutes. Furthermore, catchment export of Mg, Ca, and K was strongly connected to travel times of discharging stream water ($r = 0.78$-0.83). Conversely, increasing Na export was linked to a reduced areal proportion of mires (r = -0.79). The results suggest that a significant part (~45%) of the catchment stream export came from deep-soil weathering sources (>2.5 m). These results have implications

* Corresponding author at: Department of Forest Ecology and Management, Swedish University of Agricultural Sciences, SE-901 83 Umeå, Sweden.
E-mail address: eljs@dhigroup.com (E. Jutebring Sterte).

for terrestrial and aquatic water quality assessments. If deep soils are present, focusing mainly on the shallow soil could lead to misrepresentation of base cation availability and the acidification sensitivity of groundwater and water recipients such as streams and lakes.

1. Introduction

The water quality of catchments has recently attracted increasing attention due to concern about the effects of climate change and the increasing pressure on terrestrial and aquatic ecosystems, including the impact from forestry (Iwald et al., 2013; Nieminen et al., 2020; Xia et al., 2015). These factors are making it increasingly important to understand the hydrological and biogeochemical processes affecting water quality and their connection to water pathways and travel times (Hrachowitz et al., 2016; McDonnell et al., 2010; Weill et al., 2011). Biogeochemical processes including weathering and solute transport are affected by the pathways and travel times of water in different subsurface environments before it reaches streams and lakes (Powers et al., 2012; Tiwari et al., 2017). Due to the generally slow weathering of silicates, the relationship between hydrology and weathering are particularly important in areas without carbonate minerals in the soils. Water pathways and travel times depend on catchment characteristics including the catchment size, slope, soil type, and soil depth, as well as the impact of seasonal climatic variability (Botter et al., 2010). The effects of landscape heterogeneity on solute transport can be observed by monitoring temporal and spatial stream concentration changes between different catchments (Godsey et al., 2009; Herndon et al., 2015), which can in turn be mechanistically linked to catchment functioning (Dwivedi et al., 2019; Partington et al., 2013). However, the connection between the transport of reactive and conservative solutes to the hydrological mechanisms in catchments of different scales is not fully understood (Kirchner et al., 2000; Kolbe et al., 2020). It is therefore necessary to improve our understanding of this connection in order to reduce the uncertainties in predictive water quality modelling.

Base cations such as Mg, K, Ca, and Na, are solutes whose mobilisation and transport are especially strongly linked to catchment hydrological function due to their comparatively high mobility (Asano et al., 2006; Blumstock et al., 2015; Maher, 2010). These cations are derived partially from atmospheric deposition (Richardson et al., 2017; Wilhelm et al., 2013), but their primary source in mineral-rich areas is typically weathering (Klaminder et al., 2011a; Landeweert et al., 2001; Ouimet and Duchesne, 2005). Globally ca. 45% of the total export of solutes to the world's rivers is estimated to derive from weathering of silicate minerals (Stumm and Wollast, 1990). Protons are consumed during silicate weathering, making this process an important pH buffer in soils without carbonates. Carbonic acid is a common source of the protons consumed during weathering; consequently, weathering is an important sink for atmospheric CO_2 and has a significant impact on the carbon cycle over geological time scales, making it important in climate change discussions (Goddéris et al., 2006). Weathering is also important for terrestrial and aquatic ecosystems as a major process of acid neutralization in groundwater with significant effects on the pH of downstream recipients such as streams and lakes (Larssen and Carmichael, 2000; Watmough et al., 2014). In addition to their effects on the carbon cycle and water pH, base cations released by weathering processes are essential in many fundamental biological processes including energy storage, cell signalling, and photosynthesis (Lawlor, 2004; Zhu et al., 2016). Magnesium, K, and Ca are vital plant nutrients and are important for nucleic acid stability and biological processes such as protein synthesis (Jobbágy and Jackson, 2001; Konrad et al., 2004; Moslehi et al., 2019). Moreover, Ca is important for egg-shell formation and calcification of invertebrates' exoskeletons (Hessen et al.,

2017) and is, together with Mg, an important driver of freshwater community structures (Jeziorski et al., 2008; Weyhenmeyer et al., 2019). The weathering process and its products are thus essential for forest growth and aquatic biota (Gbondo-Tugbawa and Driscoll, 2003). An improved understanding of the temporal and spatial variation of weathering processes and their relationships with catchment hydrology and characteristics will thus be needed to better protect water resources and support sustainable land use.

Weathering rates depend on many interconnected factors that can vary in time and space, including flow rate, pH, root uptake, climatic conditions, and soil mineralogy (Drever, 1994; Stewart et al., 2001; Whitfield and Watmough, 2012). This makes it challenging to predict weathering rates on the landscape scale. Efforts to improve predictive accuracy have resulted in the development of several different on-site, laboratory, and reactive transport model methods. Weathering rates are commonly estimated using mass balance and profile-based methods, which both have their own advantages and disadvantages. Profile methods can be field (Egli and Fitze, 2000; Ouimet, 2008) and/ or model oriented (Casetou-Gustafson et al., 2019; Lebedeva and Brantley, 2020; Ouimet and Duchesne, 2005), but both types typically focus on the unsaturated zone or shallow soil where weathering rates are often assumed to be highest. Common process-based modelling tools such as PROFILE and ForSAFE have been developed and successfully used to model weathering in the root zone at many sites (Phelan et al., 2014; Sverdrup et al., 1995; Wallman et al., 2005). Preliminary efforts have been made to apply these models to catchment hydrology; notably, PROFILE was used to model the saturated flow on a homogeneous hillslope and to couple ForSAFE to the resulting two-dimensional flow map. However, current methods for modelling weathering rates on the catchment scale have several shortcomings (Erlandsson Lampa et al., 2020; Zanchi, 2016). In contrast, catchment mass balance methods estimate weathering rates on the basis of precipitation inputs and stream outputs (Ackerer et al., 2020; Joki-Heiskala et al., 2003). These methods generally assume that base cation fluxes are stable enough to provide robust annual estimates (Bricker et al., 2003; Velbel and Price, 2007). Different methods of predicting weathering rates have been found to generate highly divergent estimates (Akselsson et al., 2019; Klaminder et al., 2011b). This variability has been linked to input data uncertainties and differences in assumptions regarding the depth of the weathering zone (Futter et al., 2012). For example, Whitfield et al. (2006) demonstrated that mass balance methods can give greater estimates of catchment weathering rates than profile-based methods focusing mainly on the shallow soil because the latter methods neglect contributions from deeper soil layers.

Much of the input data needed to use mass balance and profile-based methods is site-specific and difficult to obtain (Koseva et al., 2010). It is therefore tempting to directly link weathering rates to changes in base cation concentrations in streams and stream flows (Godsey et al., 2009). Field observations have shown that the stream concentrations of base cations typically increase during low flows and decrease during high flows; this trend is known as the Q-C relationship (Abbott et al., 2018; Ameli et al., 2017; Van Meter and Basu, 2017). However, the Q-C relationship varies from element to element and stream to stream (Godsey et al., 2009; Kirchner and Neal, 2013; Moon et al., 2014). Its variation has primarily been linked to factors affecting catchment hydrology, including the catchment slope (Torres et al., 2015), the hydraulic conductivity of the soils (Gabet et al., 2006), and the soil contact time (Benettin et al., 2015; Maher, 2010). It has also

been suggested that higher base cation concentrations are connected to soil depth (Bouraoui and Grizzetti, 2011). Additionally, model studies have associated deeper groundwater with higher base cation concentrations, which, in turn, have been linked to older waters (Abbott et al., 2016; Jutebring Sterte et al., 2021a; Kolbe et al., 2020). However, the dependence of weathering of different elements on factors controlling hydrology is not yet fully understood. Connecting weathering models to models that describe surface and groundwater flow in a 3D space would enable analysis of factors controlling the hydrology, deep-soil base cation sources, and variations in stream concentration in different sub-catchments. Such a combined model could complement existing methods for studying large-scale weathering patterns and provide new insights into the connection between hydrology, soil depth, and solute transport. However, to test this approach to modelling weathering one would need to identify a catchment with deeper mineral soils for which a well-established flow model exists and for which there is ample empirical data on both flows and weathering.
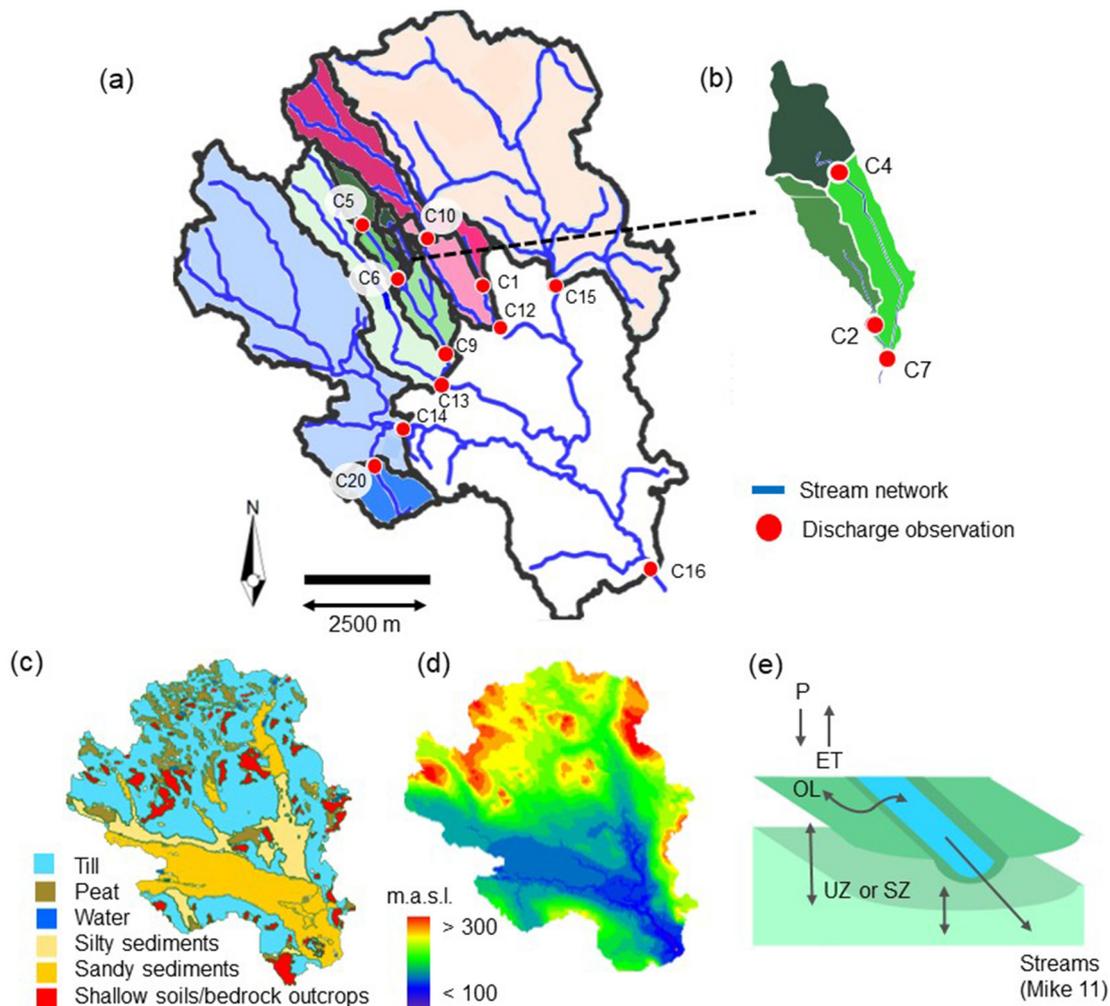
One such catchment is the Krycklan catchment in the boreal region of northern Sweden (Laudon et al., 2013). The catchment consists of a forested landscape with intertwined mires, lakes and streams and has long data sets that can be used to study its hydrology and geochemistry. A 3D flow model called Mike SHE that accounts for streamflow, overland flow, and saturated and unsaturated subsurface flow was developed, calibrated, and validated for 14 of the Krycklan sub-catchments (Jutebring Sterte et al., 2018, 2021a). The Krycklan site and its established flow model provided a testbed for investigating the connection between weathering of deep mineral soils, the catchment's hydrological functioning, and soil contact time on different scales. The study focused on the four most important base cations, Mg, Na, K, and Ca, with the aim of clarifying the relationship between weathering and solute transport and their connection to catchment hydrology, including water travel time and catchment characteristics.

2. Method

2.1. Study site and flow model

The Krycklan catchment is situated in northern Sweden, at the boundary between the temperate and subarctic climatic zones. Its landscape is typical of the boreal region, featuring a forest on mineral soil with several peat mires. The forest is dominated by Norway spruce (*Picea abies*) and Scots pine (*Pinus sylvestris*) (Laudon et al., 2021b; Laudon and Sponseller, 2018). The topography spans elevations from 100 to 400 m.a.s.l. with higher altitudes to the northwest and lower altitudes to the southeast (Fig. 1). The main soil type at higher altitudes is glacial till, which reaches depths of up to 20 m (Bishop et al., 2011;

Fig. 1. The Krycklan catchment. (a) Sub-catchment locations and stream network. Stream observation stations are indicated by red circles. (b) Sub-catchments C2, C4, and C7. (c) Soil types in the catchment based on a soil map (1:100,000) from the Swedish Geological Survey (2016) and field investigations. (d) Surface topography in meters above sea level. (e) Schematic representation of the Mike SHE flow model. The model includes evapotranspiration (ET), precipitation (P) (rain and snow), overland flow (OL), unsaturated flow (UZ), and saturated flow (SZ). All parts can interact at each time step and are fully integrated with the streams (modelled using Mike 11), as described in Supplement A. (For interpretation of the references to colour in this figure legend, the reader is referred to the web version of this article.)

Nyberg, 1995; Seibert et al., 2009). The main soil types at lower altitudes are silty-clay and sandy sediments, and the soil deposits can be up to at least 50 m deep. Field studies have shown that the main constituents of the mineral soil are quartz (47%), plagioclase (26%) and K-feldspar (20%). Smaller quantities of apatite (0.2%), biotite (0.6%), hornblende (5.3%), and pyroxene (1.0%) have also been found (Erlandsson Lampa et al., 2020; Nyberg et al., 2001). Streamflow, groundwater levels, and water quality in the catchment have been monitored for over 30 years, with the longest data set commencing in the 1980s. The catchment is divided into 14 sub-catchments with different scales and landscape characteristics, which are designated C1 to C20 (Fig. 1, Table 1).

In this study, the catchment's hydrology was described using a previously developed Mike SHE/Mike 11 flow model (Jutebring Sterte et al., 2018, 2021a). This 3D flow model calculates the groundwater and surface water flows using topography, vegetation and soil properties, and time-varying climate inputs (Fig. 1, Table 1). For each time step, the model calculates water fluxes between the ground surface, subsurface, and streams throughout the catchment. Processes included are saturated and unsaturated flow, overland flow, evapotranspiration, and snowmelt. Streams are modelled with the 1D modelling tool Mike 11, which is coupled and fully integrated with Mike SHE. The flow model includes the whole Krycklan catchment and extends past the bedrock

beneath the soil deposits. The input data span the period from 2009 to 2014. A more detailed description of the flow model and its updating are presented in Supplement A and Jutebring Sterte et al. (2018, 2021a).

2.2. Weathering model

A weathering model was integrated with the hydrological flow model of the catchment, as described in Supplement A (Jutebring Sterte et al., 2018, 2021a). In the resulting flow and weathering model, solutes are transported by advection according to the established flow field. New concentrations are calculated for each cell and each time step. The solute concentration can be changed by pre-established sources, by mixing, or by reactions controlled by an external module called Mike ECO Lab, (Supplement B, Butts et al., 2012). We used the Mike ECO Lab model to describe the weathering of base cations in the flow and transport model. This study was divided into three main phases: 1. Calibration of weathering rates, 2. validation of the coupled hydrology and weathering model, and 3. analysis of catchment export.

The flow model used in this study has two main sources of base cations: precipitation and weathering, which are described using Mike ECO Lab. The precipitation concentration (C_p) is set to an average value based on field observations (Table 1). Weathering was permitted in

Table 1

Catchment characteristics and chemistry. (a) Catchment characteristics (see also Fig. 1). (b) Average observed stream concentrations of Mg, K, Ca, and Na, 2009-2014. The table also includes the average pH of the sub-catchment streams of Krycklan for the same period. (c) Average observed groundwater concentration in the mineral soil. Chemical data can be acquired from the Krycklan Database (2013).

Catchment	(a) Catchment characteristics						(b) Average observed stream chemistry				
	Catchment size	Till	Mire	Sorted sediments	Lakes	MTT*	Mg	K	Ca	Na	pH
	(km²)	(%)	(%)	(%)	(%)	(year)	(mg l⁻¹)	(mg l⁻¹)	(mg l⁻¹)	(mg l⁻¹)	(-)
C1	0.5	91	0	0	0.0	1.3	0.8	0.5	2.2	1.7	5.3
C2	0.1	79	0	0	0.0	0.8	0.7	0.3	1.8	1.6	5.0
C4	0.2	29	42	0	0.0	0.8	0.4	0.3	1.1	0.9	4.4
C5	0.7	47	46	0	6.4	0.8	0.4	0.2	1.2	0.8	4.8
C6	1.1	51	29	0	3.8	0.9	0.7	0.4	1.9	1.3	5.4
C7	0.5	68	16	0	0.0	1.1	0.7	0.4	1.9	1.4	4.9
C9	2.9	64	14	11	1.5	1.4	0.8	0.5	2.4	1.6	5.7
C10	3.4	64	28	1	0.0	1.1	0.6	0.5	1.9	1.4	5.2
C12	5.4	70	18	6	0.0	1.3	0.7	0.5	2.1	1.4	5.5
C13	7.0	60	10	18	0.7	1.4	0.8	0.5	2.4	1.5	5.6
C14	14.1	46	6	39	0.7	2.4	0.9	0.8	3.0	1.6	6.2
C15	19.1	64	15	10	2.4	1.5	0.8	0.6	2.7	1.5	6.3
C16	67.9	51	9	31	1.0	2.3	1.1	0.9	3.3	1.7	6.5
C20	1.5	55	9	28	0.0	2.7	1.1	1.0	5.0	1.7	6.4

	(c) Observed groundwater concentrations									
Well location	Well ID	Depth below ground (m)	No.	Magnesium (Mg)		Potassium (K)		Calcium (Ca)		Sodium (Na)	
				(mg l⁻¹)	STDEV	(mg l⁻¹)	STDEV	(mg l⁻¹)	STDEV	(mg l⁻¹)	STDEV
	201	3	4	1.3	0.2	1.1	0.1	4.2	0.9	2.7	0.2
	212	20	1	4.1	–	4.6	–	12.5	–	4.8	–
	213	48	2	4.3	1.1	3.0	0.5	15.7	2.5	8.1	3.6
C2	S -transect	<2	220	0.5	0.3	0.3	0.2	1.4	0.8	2.0	0.6
	301	4	4	1.0	0.2	1.0	0.2	2.5	0.4	2.3	0.1
	302	2	3	0.5	0.0	0.5	0.1	1.6	0.1	1.9	0.1
	303	5	4	2.7	0.1	2.5	0.2	7.7	0.3	3.1	0.2
	304	11	4	2.7	1.3	1.9	0.7	9.5	4.4	3.3	0.9
	401	3	4	2.0	0.4	2.0	0.9	6.4	0.7	3.2	1.0
	402	2	1	0.9	0.0	1.5	0.0	1.7	0.0	3.8	0.0
C7	403	4	4	1.7	0.0	1.1	0.3	5.8	0.2	3.0	0.1
	404	10	4	3.3	0.1	3.0	0.1	10.1	0.3	4.0	0.2
	411	15	3	2.8	0.1	2.1	0.1	10.5	0.4	3.6	0.1
	412	25	3	4.3	0.1	2.4	0.2	16.8	0.5	4.8	0.0
C9	501	4	3	3.3	0.1	2.4	0.0	11.7	0.3	4.0	0.1
	511	5	3	2.3	0.5	2.4	0.2	10.3	2.4	6.2	2.8
C13	601	6	5	1.7	0.3	1.4	0.1	5.7	0.8	2.1	0.4
Deep**	C_{eq}	≥15	9	3.8	0.8	2.7	0.8	14.0	2.8	5.1	0.4
Prec.***	C_p	–	–	0.03		0.12		0.11		0.15	

* Annual mean travel time (MTT) values as calculated in Jutebring Sterte et al. (2021a).

** Average concentrations of four different wells located in C2 (212 and 213) and C7 (411 and 412), with depths ranging from 15 to 50 m below the ground. In total, nine samples were taken from these wells between 2012 and 2018.

*** C_p values are long term volume-weighted averages from April 2002 to September 2018 based on monthly bulked data for the Krycklan site.

the unsaturated and saturated groundwater of the mineral soil and started as soon as water infiltrated the soil surface. Consequently, no weathering was allowed for surface waters or groundwaters in mires (Fig. 2). However, mires, lakes, and streams could still receive base cations from the surrounding area or by precipitation. A simple and widely utilised model was used to calculate primary weathering rates for sub-surface flow (Ameli et al., 2017; Drever, 1994; Maher and Druhan, 2014). The concentration (C) in time step t was calculated as a function of the concentration in the preceding time step and the weathering rate (R):

$$C^t = C^{(t-1)} + R\left(C^{(t-1)}\right)dt \tag{1}$$

To estimate the weathering rate (R, mg l^{-1} day^{-1}) for minerals, we used an equation based on the Transition State Theory (TST-style) that was previously used to calculate weathering rates (Ameli et al., 2017; Erlandsson et al., 2016; Goddéris et al., 2006; Maher et al., 2009). According to this theory, the weathering rate for a mineral close to the equilibrium concentration (Ceq_x) is slower than when it is far from equilibrium (Schott et al., 2009):

$$R\left(C^{(t-1)}\right) = R_{max}\left(1 - \frac{C^{(t-1)}}{C_{eq}}\right)^b \quad \left(\text{mg l}^{-1}\,\text{day}^{-1}\right) \tag{2}$$

In the TST-style equation, the weathering rate R depends on the maximum weathering rate (R_{max}), the concentration at the time (C^{t-1}), the equilibrium concentration (C_{eq}), and a brake-constant b. In the TST-style model, b defines the shape of the weathering rate curve. For example, if $b = 0$, then the weathering rate is constant (R_{max}), resulting in a linear relationship between groundwater travel time and base cation concentration. However, weathering does not depend only on the soil contact time and cannot often be described by a linear relationship. The process depends on numerous additional factors, including temperature, pH, and geochemical and biological processes (Anderson et al., 1997; Bishop et al., 2011; Whitfield et al., 2006). These factors are averaged into the two variables of R_{max} and b in Eq. (2), resulting in a non-linear relationship. R_{max} and b can take different values for different sites and minerals, and must be calibrated using field data or be theoretically derived (Erlandsson et al., 2016). Thus, although the model does not include actual thermodynamic calculations or expressions for the weathering of specific minerals, it is still flexible enough to describe different types of weathering kinetics based on empirically calibrated constants. It was hypothesized that when used in combination with a full-scale 3D representation of the catchment's hydrology, this model would be sufficient to explain much of the variation in base cation concentrations throughout the landscape.

2.2.1. Step 1: calibration of weathering rates

The maximum weathering rate (R_{max}) and the shape constant b (Eq. (2)) were calibrated separately for each of the four base cations Mg, K, Ca, and Na, using an automatic calibration routine (Supplement B) in which the model was repeatedly used to simulate a single hydrological year (2010) until stable groundwater concentrations were achieved for each set of R_{max} and b values. The modelled groundwater concentrations were then compared to the groundwater concentrations observed at numerous wells throughout the Krycklan catchment in 2010 (Table 1). The R_{max} and b values that gave the concentrations closest to the observed values were used in steps 2 and 3. The empirical data were collected from wells in the mineral soils at five different sites and different soil depths (Table 1). Sampling was conducted during two projects: *S-transect groundwater monitoring* (base cation data for the years 2006 and 2007) and *Snowcat groundwater monitoring* (base cation data for the years between 2012 and 2018) (Laudon et al., 2013). The S-transect studied in the first project is located close to the stream of C2 (Fig. 1). During this project, lysimeters were placed between 4 m and 22 m from the stream at various depths <2 m below the ground surface, focusing on the soil's upper horizons. During the sampling period at this site, about 220 measurements of base cation concentrations were acquired. The Snowcat groundwater monitoring project focused on deeper groundwater wells throughout the Krycklan catchment (up
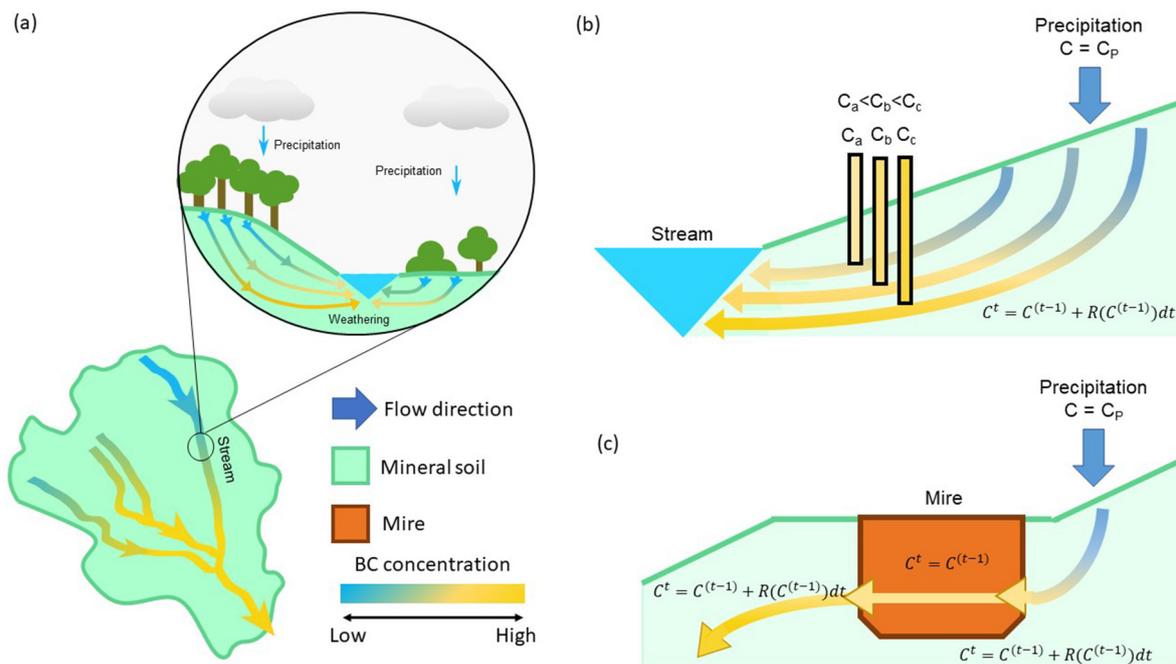
Fig. 2. Schematic figure over the conceptual model of weathering in the mineral soil. (a) Schematic figure connecting increasing base cation (BC) concentration in the stream network to soil contact time. Streams receive groundwater with increasing concentration due to weathering in the mineral soil. (b) Weathering in the mineral soil. At each time step, the solute is transported by advection. The concentration in each cell is then adjusted using the weathering equation (Eq. (2)). The result is that older waters are associated with higher base cation concentrations. (c) No weathering occurs in the mires, lakes, or streams, but they can receive nutrients from the surrounding mineral soils or through precipitation (C_p, Table 1).

to 50 m below the ground surface). These were measured once in 2012 and then once per year from 2015 to 2018. Although the measurements are sparse, they are relatively stable and provide information on concentrations at depths below 2 m in the mineral soil. The equilibrium concentration (C_{eq}) was taken as the average from the four deepest wells (deeper than 15 m).

2.2.2. Step 2: validation of coupled hydrology and weathering model

After calibrating R_{max} and b against the observed groundwater concentrations, the model was tested by comparing the observed and modelled stream concentrations. The model was run from 2009 to 2014, calculating daily stream concentrations. Empirical measurements for the same period were available with weekly to monthly frequencies for the 14 tested sub-catchments (Table 1). Statistical evaluations were performed by comparing the modelled and observed values for the same date. The model's performance was evaluated on seasonal and annual time scales for all 14 sub-catchments (Table 1). The annual evaluations included all months and days with available observations. Three distinct seasons in Krycklan were evaluated: winter, spring, and summer. As in our previous work (Jutebring Sterte et al., 2021a), winter was defined as the period from early December to late February. In winter, the air temperature was below 0 °C and precipitation accumulated as snow, so no input to the groundwater occurred. Spring was defined as the period from April to May, when air temperatures started increasing and the main part of the snowmelt occurred. Summer was defined as the period from July to September, during which the catchment's hydrology was affected by relatively high air temperatures and high ET. Data for March, June, October, and November were excluded when calculating seasonal averages because they are transition months between the otherwise relatively distinct seasons.

2.2.3. Step 3: catchment export investigation

The export of base cations to the streams was calculated as the product of the flow rates predicted by the model and the concentrations predicted by the model. The predicted average annual export values for the different sites were compared to catchment characteristics previously found to have important effects on streamflow and stream chemistry (Jutebring Sterte et al., 2021a; Karlsen et al., 2016; Klaminder et al., 2011b) including the areal proportion of mires and lakes, the mean travel time (MTT) of the stream water contribution, and the catchment size (Table 1). The objective was to find the primary factors controlling catchment export of base cations in the different sub-catchments and to determine whether any of the base cations responded differently to changes in these factors. The model also provided a unique opportunity to assess the relative contributions of deep and shallow weathering because it distinguished between solutes weathered above the lower level of the first saturated computational layer (<2.5 m depth) and those weathered in deeper soils. As mentioned in the introduction, it has been suggested that reliance on potentially inaccurate assumptions

about weathering zone depth may partly explain why estimated weathering rates obtained using mass balance methods diverge from those obtained using methods focusing mainly on the shallow soil (Futter et al., 2012; Whitfield et al., 2006). The model presented herein made it possible to assess the importance of deep-soil weathering of the different base cations as well as differences in the exports of different catchments.

3. Results

3.1. Step 1: calibration of weathering rates

During the calibration process, the model was run repeatedly with different sets of R_{max} and b values. Each such parameterisation was then evaluated by comparing the stable concentrations predicted by the model to the empirically observed groundwater concentrations (Table 1). When calibrating against the groundwater data, all four base cations ended up with a b constant >0; Na and Mg had the largest b constants ($b_{Na} = 4.0$, $b_{Mg} = 2.9$) and Ca and K the lowest ($b_{Ca} = 0.3$, $b_K = 0.4$). R_{max} was calibrated to 4.0×10^{-3} mg l^{-1} day^{-1} (Mg), 2.0×10^{-3} mg l^{-1} day^{-1} (K), 7.0×10^{-3} mg l^{-1} day^{-1} (Ca), and 5.5×10^{-2} (Na) mg l^{-1} day^{-1}. The strongest correlations between calculated and observed concentrations were found for Mg and Ca ($r_{Mg} = 0.77$, Fig. 3a, $r_{Ca} = 0.84$, Fig. 3c), while Na exhibited the weakest such correlation ($r_{Na} = 0.64$, Fig. 3d). The model underestimated high groundwater Mg and K concentrations and overestimated low K and Mg concentrations when compared to the empirical data, but the overall ME was low for these cations ($ME_{Mg} = 0.1$ mg l^{-1} and $ME_K = 0.1$ mg l^{-1}). Additionally, low Ca concentrations were underestimated and high Ca concentrations were overestimated, with a somewhat larger ME ($ME_{Ca} = 1.4$ mg l^{-1}). Most of the calculated Na concentrations between 2 mg l^{-1} and 4 mg l^{-1} were clustered around the 1:1 trend corresponding to perfect agreement with the empirical observations, and the overall ME for Na was low ($ME_{Na} = 0.1$ mg l^{-1}). The lowest MAE and RMSE values were found for K (MAE = 0.4 mg l^{-1} and RMSE = 0.5 mg l^{-1}) and the largest for Ca (MAE = 2.3 mg l^{-1} and RMSE = 2.9 mg l^{-1}).

3.2. Step 2: Validation of coupled hydrology and weathering model

In step 2, the model was run for the whole period from 2009 to 2014 and validated by comparing the predicted weathering rates to empirical observed stream concentration data. The following discussion focuses on the time series data obtained for Ca, which was the dominant base cation in the studied streams, and on four sub-catchments with distinct properties: C2 (a small till dominated catchment), C4 (a small mire dominated catchment), C20 (a small silt dominated catchment), and C16 (the main catchment outlet). C2 and C4 were previously found to have relatively short yearly mean travel times, while C20 and C16 have relatively long yearly mean travel times (Table 1). Time series
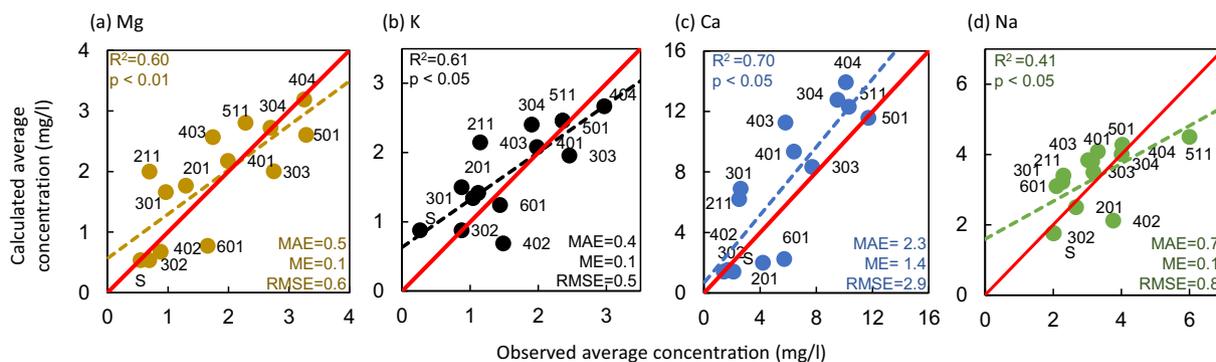
Fig. 3. Modelled groundwater concentrations for the calibrated sets of R_{max} and b values. (a) to (d) calculated concentrations compared to average observations for Mg, K, Ca, and Na, respectively. The red line indicates a perfect match between the model and the empirical observations (i.e., a 1:1 trend line), the dashed line is the regression, and each dot shows the average calculated and observed concentrations for an individual groundwater well (Table 1). Key statistical values for the regressions are also shown.

data for the other base cations in the same representative sub-catchments are presented in Supplement C.

Modelled and observed concentrations were not captured very well on a daily time scale, and the correlation was generally weaker for the smaller sub-catchments with shorter travel times (e.g., C2 and C4, Fig. 4a and b). Evaluation of the model's output is complicated by the fact that its temporal resolution is greater than that of the observations, which may therefore not capture the full variability of stream chemistry. Since different types of water (e.g., mire water and deep groundwater) can differ considerably in terms of base cation concentrations, evaluations of the model's performance will inevitably be highly sensitive to the timing of the stream water sampling and the model's ability to accurately predict the timing of hydrological episodes. For example, short-lived inputs from the mire in spring and summer caused a large spread

of concentrations in C20, which was not reflected in the observations (Fig. 4c). This does not necessarily mean that the modelled variation in concentration does not occur; it is possible that it would not be seen due to the lower temporal resolution of the stream chemistry measurements. Whenever there was a precipitation event, the water flow from the mires exceeded the baseflow from the silty soils, resulting in a fluctuating concentration pattern. However, the model successfully captured the general Q-C relationships for the different sub-catchments (Fig. 4, Supplement C). In general, Ca concentrations were higher during low flows (winter and high summer ET) and lower during high flows (snowmelt and precipitation events) in all investigated sub-catchments. The lowest predicted concentrations and flows were found in the small catchments C2 and C4, and the mire-dominated sub-catchment (C4) had lower concentrations than the till-dominated

Fig. 4. Representative modelled and observed concentration time series for Ca. The left-hand figures in rows (a) to (d) show the modelled and observed Ca stream concentrations (left y-axis) in four representative catchments: C2, a small till-dominated catchment; C4, a small mire-dominated catchment; C20, a small silt-dominated catchment; and C16, the main catchment outlet. Note that the model calculates daily discharges and concentrations, while observations were made less frequently. The right-hand figures in rows (a) to (d) show the Q_{model}-C_{model} and the $Q_{observed}$-$C_{observed}$ relationship for the same four catchments on all dates on which observations were made. Note that the x-axis shows the specific discharge on a logarithmic scale. Additional figures for Mg, K, and Na are presented in Supplement C.

sub-catchment (C2), in agreement with the observations. The highest concentrations were found in the sub-catchments with longer travel times, i.e., C16 and C20.

The average modelled seasonal and annual concentrations correlated strongly with the corresponding observations. Generally, the best fits were found for the winter season (Fig. 5). For all seasons, the model's performance was relatively good for Ca ($r = 0.89$-0.93, $p < 0.05$, Fig. 5), Mg ($r = 0.90$-0.95, $p < 0.05$, Fig. 5) and Na ($r = 0.80$-0.89, $p < 0.05$, Fig. 5), but poorer for K ($r = 0.75$-0.87, $p < 0.05$, Fig. 5), and especially for the high K concentrations in early spring. The average modelled Mg concentrations were close to the observed values but slightly overestimated (ME = 0.03-0.07 mg l^{-1}, MAE = 0.06-0.12 mg l^{-1}, Fig. 5). Calcium concentrations tended to be overestimated, especially in the smaller sub-catchments, and were

underestimated in catchments with longer travel times such as C16 and C20 (ME = 0.17-0.56 mg l^{-1}, MAE = 0.32-0.64 mg l^{-1}, Fig. 5). Similar trends across sub-catchments were observed for Mg, Ca, and K (Fig. 5): their concentrations were generally overestimated in smaller sub-catchments and underestimated in concentrations with longer travel times. The behaviour of Na differed from that of the other base cations: in all seasons, its concentrations were slightly higher in some sub-catchments with no apparent dependence on size or MTT (ME = 0.16-0.31 mg l^{-1}, MAE = 0.24-0.41 mg l^{-1}, Fig. 5).

3.3. Step 3: catchment export analysis

The average annual catchment export through streams could be calculated from the flows and concentrations predicted by the model. The
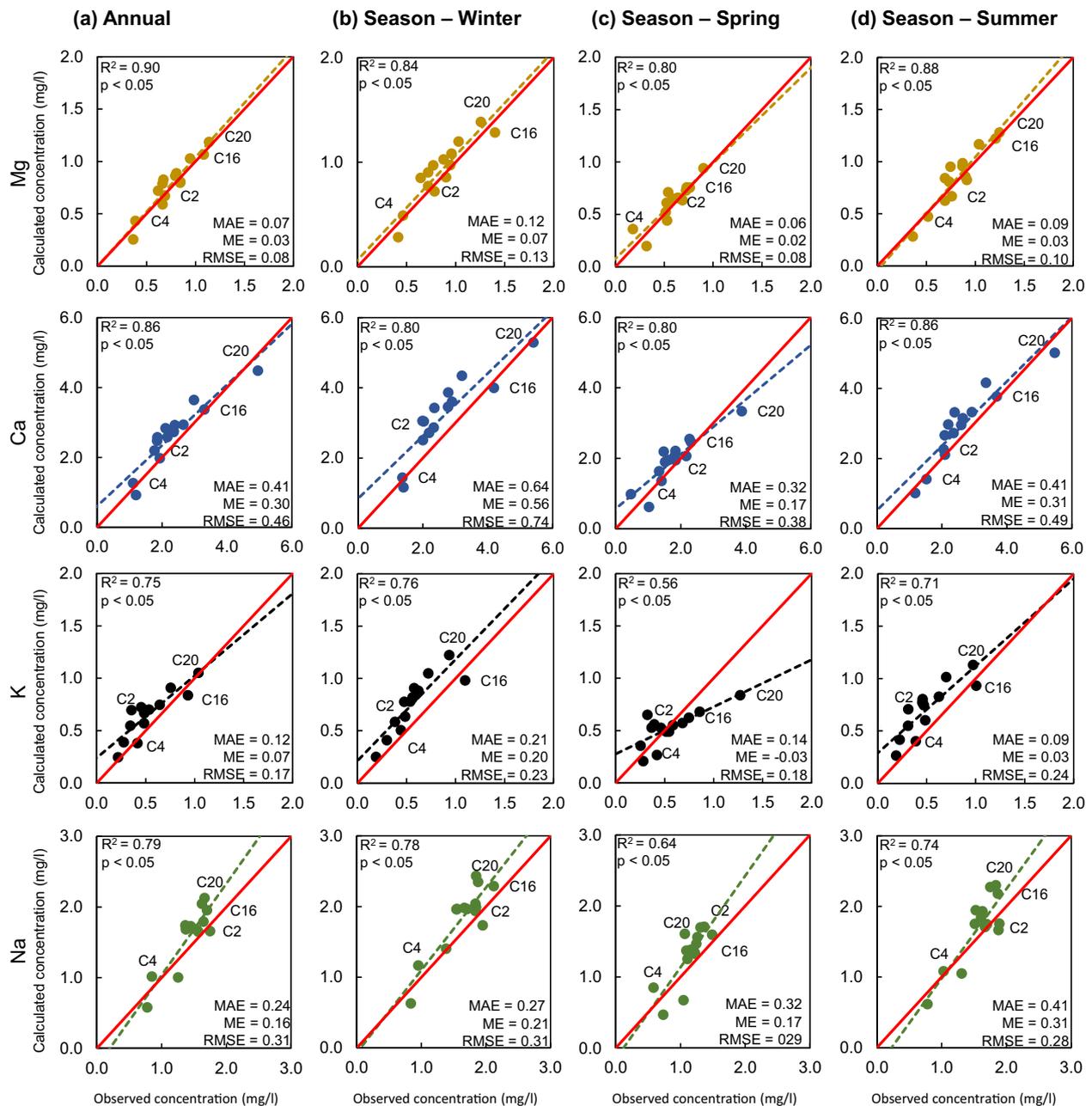
Fig. 5. Model results, seasonal averages. The figure compares calculated and observed annual and seasonal (winter, spring, and summer) average concentrations (mg l^{-1}) of the four base cations: Mg (yellow), Ca (blue), K (black) and Na (green). The averages are based on the dates when observations were made. Results for all 14 sub-catchments are included. Regressions are shown using dashed lines and the 1:1 trend corresponding to perfect agreement between the calculations and the observations is shown using a solid red line. Seasonal data for individual sub-catchments can be found in Supplement C. (For interpretation of the references to colour in this figure legend, the reader is referred to the web version of this article.)

total base cation export in individual sub-catchments varied between 0.04 eq m^{-2} year^{-1} and 0.11 eq m^{-2} year^{-1} (Fig. 6), and the average export values for the four individual base cations ranged from 0.01-0.03 eq m^{-2} year^{-1} for Na, 0.004-0.007 eqm^{-2} year^{-1} for K, 0.01-0.06 eq m^{-2} year^{-1} for Ca, and 0.02-0.03 eq m^{-2} year^{-1} for Mg (Fig. 6a). Smaller mire-dominated sub-catchments (e.g., C4) had the lowest export values, while silt-dominated sub-catchments (e.g., C16 and C20) had the highest export values. The results indicated that approximately 50-70% of the weathering occurred in the shallow part of the soil (< 2.5 m depth). However, on average, 45% of the base cation export (0.01-0.06 eq m^{-2} year^{-1}) originated from deep-soil sources. Specifically, deep soil exports of Mg, K, Ca, and Na accounted for 10%, 5%, 25%, and 5% of the total base cation export, respectively. Interestingly, the contribution of deep-soil weathering to overall export varied between the base cations: it was 30-60% for Mg, 20-50% for K, 40-70% for Ca, and 10-30% for Na, depending on catchment. The relative contributions of deep-soil weathering reflected the way weathering rates decreased with soil depth for the different base cations. For example, the weathering rate of Na decreased more rapidly with soil depth than those of the other base cations (Fig. 6b). Na was also the base cation showing the least export from deep soils.

No strong connection between catchment export and catchment size was found. However, there was a strong positive correlation between MTT and total base cation export ($r_{Bc} = 0.77$, $r_{BC\_Deep} = 0.86$, $p < 0.05$, Table 2). This correlation was especially pronounced for Mg, K and Ca ($r_{Mg} = 0.78$, $r_K = 0.78$, $r_{Ca} = 0.83$, Table 2, $p < 0.05$) but was weaker for Na ($r_{Na} = 0.57$, $p < 0.05$). Likewise, there was a strong positive correlation between the total base cation export and the average stream pH ($r_{Bc} = 0.80$, $r_{BC\_Deep} = 0.87$, $p < 0.05$, Table 2). Upon separating the base cations, the correlation remained strongest for Mg, Ca, and K ($r_{Mg} = 0.83$, $r_K = 0.73$, $r_{Ca} = 0.84$, $p < 0.05$, Table 2). Moreover, Na was the base cation most strongly linked to a catchment's proportion of mires and lakes ($r = -0.79$, $p < 0.05$, Table 2).

4. Discussion

Within the relatively small Krycklan catchment (68 km^2), there is considerable variation in the base cation concentrations in different parts of the stream network (Fig. 5). The release of base cations and their subsequent transport through the landscape involves complex interactions between hydrological, geochemical, and biological processes. However, the present model suggests that a thorough understanding of hydrology can explain much of the spatial and temporal variation in base cation concentrations. In contrast to common modelling approaches (Augustin et al., 2016; Koseva et al., 2010) that combine relatively simple hydrology models with complex weathering routines, we used a thoroughly calibrated 3D distributed hydrological model combined with a comparatively straightforward weathering model to quantify weathering on a landscape scale. Our modelling approach accounted for the dynamics of water flow, transport, and weathering in time and space, enabling simultaneous investigation of weathering in sub-catchments of different sizes and characteristics. The weathering model's constants were calibrated for different solutes, but the same model was then applied throughout the catchment to all soil depths and all soil types except peat. The resulting calculations agreed well with the observations on both annual and seasonal time scales for all sub-catchments, indicating that the combination of a relatively simple weathering model with a well-calibrated 3D flow model may be sufficient (or if not, may provide a robust starting point) for predicting weathering rates and solute transport across catchments.

4.1. Model evaluation

The calibration of the weathering model was based entirely on empirical observations of the groundwater chemistry throughout the Krycklan catchment. More specifically, the assumed equilibrium concentration for each base cation (C_{eq}) was fixed based on observed concentrations in deep groundwater (>15 m, Table 1). However, it is unlikely that the sampled groundwater represented the true equilibrium concentrations; higher concentrations could have been present in groundwater somewhere else in the catchment. However, both practical and theoretical limitations needed to be considered. Budget constraints limited the spatial resolution of deep groundwater sampling. Nevertheless, relatively large numbers of groundwater samples were collected from different depths and soil types throughout the catchment; this together with the catchment's rather mineralogically homogeneous soils ensured that the sampled groundwater chemistry adequately represented the area (Lidman et al., 2016).

It is also challenging to define an equilibrium concentration for the base cations because mineral solubility is typically linked to the fate of other constituents with more complex geochemistry (Sharpley, 1991). The groundwater concentrations of Al and Si, for example, are limited by various secondary phases (Maher et al., 2009; McLean, 1976). Therefore, the different mineral weathering rates will be important for determining how much of the different base cations will be released before saturation is reached. For example, if large amounts of Al and Si are released from an easily weathered mineral, the dissolved concentrations of other more weathering-resistant silicate minerals will be pushed
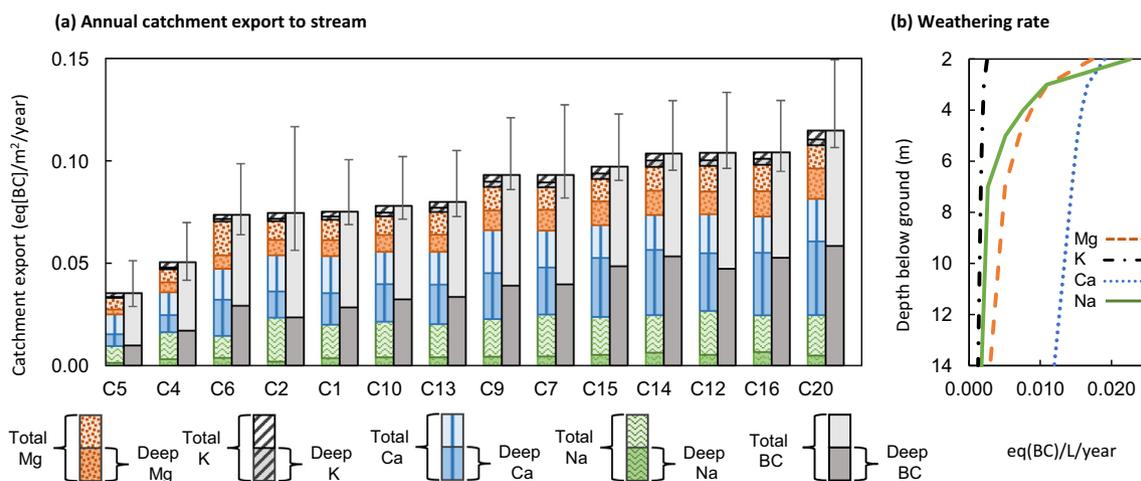
Fig. 6. Catchment export to streams and weathering rates. (a) Calculated annual average catchment export to streams in rising order. Both total export and export originating from deep weathering sources (>2.5 m) are shown, along with the minimum and maximum annual base cation export. (b) Average annual till soil weathering rate for each base cation as a function of soil depth.

closer to saturation, further reducing their weathering. In the case of Krycklan, Erlandsson et al. (2016) observed saturation with respect to both plagioclase and K-feldspar when applying a multicomponent kinetic weathering model to soils in the Krycklan catchment, suggesting that the concentrations of K and Na observed in the deep groundwater may be close to their respective maximum values. Calcium is more difficult to assess, since it is present in several minerals, all of which could contribute significantly to its presence in the groundwater, e.g., plagioclase, hornblende, and apatite. The situation is similar for Mg. The stoichiometry, solubility, and reaction kinetics of these minerals are not known in detail, which poses a challenge when assessing the weathering of their constituent elements using mineral-specific weathering rates (e.g., Erlandsson et al., 2016). Ultimately, however, it may not be crucial to get the equilibrium concentrations exactly right when applying the more simplistic approach used in this study because their purpose in the model is only to decrease the weathering rates by an appropriate amount (Eq. (1) and (2)). Calibration of the b constant (Eq. (2)) allowed for some flexibility in the choice of C_{eq}, so only reasonably accurate groundwater concentrations were needed to achieve good model performance. The validity of the approach should therefore be evaluated on the basis of the model's predictive power (Figs. 4 and 5).

The calibrated weathering model reproduced the stream concentrations for the four base cations well on both annual and seasonal time scales. It accurately captured variations in stream concentration in sub-catchments with different characteristics, including the generally low concentrations of C4 and the high concentrations of C20 (Figs. 4 and 5). The best fits to observed stream concentrations were achieved for Mg, Ca, and Na, whereas the fit for K was less good (Fig. 5). The strong seasonal correlation between the model's results and observations suggested that stream concentrations of base cations depend primarily on catchment hydrology and various catchment characteristics on different time scales. However, some variations on the daily time scale were not captured. The model predicted daily stream concentrations more accurately for larger sub-catchments with higher MTT values and smoother temporal shifts in discharge and stream chemistry (e.g., C16) than for sub-catchments with shorter MTT and more rapid fluctuations (e.g., C2 and C4). The deviations could be linked to changes in water flow or biogeochemical processes not captured on a daily time scale.

The flow model's output correlated strongly with the observed stream flows (Fig. 4 and Supplement A). However, inaccuracies in the model's predicted timings and discharge values could reduce the accuracy of the predicted concentrations, which could be critical since concentrations were not measured daily. For example, if the timing of a peak flow was off by just one day in the hydrological model, the weathering model would probably predict an incorrect concentration for that day because its prediction would be based on inaccurate information on the type of water entering the stream. Such inaccuracies could be taken to indicate poor predictive ability on the part of the

weathering model even if it actually reproduced the C-Q relationship well for all sub-catchments (Fig. 4 and Supplement C). The accuracy of daily concentration predictions could potentially be improved by reducing the daily flow model's time step or reducing the horizontal grid size. Such changes may be useful if aiming to predict concentrations over very short time scales. However, they would also increase the model's computational cost. The model's performance was considerably better on annual and seasonal time scales, which are in our opinion the most important time scales for applications of such models (Fig. 5). The generally strong relationship between the predicted and observed base cation concentrations (especially Ca, Mg, and Na) suggests that the noticeable deviations between prediction and observation for spring K concentrations are probably linked to biogeochemical processes not included in the current weathering model rather than the model's representation of the catchment's hydrology. The calculated annual catchment export to streams (Fig. 6) was also similar to previous estimates by Erlandsson et al. (2016), who estimated the export to be approximately 20 meq m^{-2} year^{-1} for Mg, 5 meq m^{-2} year^{-1} for K, 30 meq m^{-2} year^{-1} for Ca, and 30 meq m^{-2} year^{-1} for Na using mass balances of observed flows and concentrations in the C2 catchment. For comparative purposes, in this work the export of individual base cations from C2 to streams was predicted to be 17 meq m^{-2} year^{-1} for Mg, 4 meq m^{-2} year^{-1} for K, 30 meq m^{-2} year^{-1} for Ca, and 23 meq m^{-2} year^{-1} for Na (Fig. 6). The good agreement between the model's predictions and previous estimates increased confidence in the model's predictive power on an annual time scale.

4.1.1. Magnesium and calcium

The correlation between Mg and Ca catchment export to MTT was strong ($r > 0.7$, $p < 0.05$, Table 2). However, the Mg weathering rate in Krycklan seemed to decrease faster than the Ca weathering rate (Fig. 6). The model also captured this fact since the brake-constant b became larger for Mg than Ca during calibration. The main Mg source in these soils is believed to be hornblende, which can also be a significant source of Ca (Erlandsson et al., 2016). Therefore, the general similarities between Ca and Mg throughout the landscape would be consistent with hornblende weathering being a major source of both cations. Pyroxene is also present in the soils and could contribute to both Ca and Mg, although its stoichiometric composition in these soils remains unclear. However, considerable amounts of Ca can also be expected to be released from other Ca-rich minerals such as plagioclase and apatite, which are poor in Mg. Even when the Mg release was dampened, Ca concentrations increased continuously with soil depth and soil contact time. These results indicate that some mineral containing Ca but not Mg acts as a source of Ca in deep groundwater; potential candidates include apatite and Ca-rich forms of pyroxene or plagioclase.

On both annual and seasonal time scales, the weathering model predicted Mg and Ca concentrations well for the Krycklan streams (Fig. 5). However, some deviations between observations and calculations can

Table 2
Correlation matrix (r). The table shows the catchment export (eq m^{-2} year^{-1}) of all sub-catchments and their correlation to the different catchment characteristics (Table 1). The catchment characteristics include mean travel time (MTT, year), log catchment size (Log A, km^2), the proportion of mires and lakes (M & L, %), and average pH (Table 1). The matrix includes the total average export (Total BC) and the export originating from deeper soils (Total BC deep, >2.5 m). The correlation coefficient r is shown in the table. R^2 values >0.5 are shown in bold and results significant at the p < 0.05 level are labelled with an asterisk: *.

	r	MTT	Log A	M & L	pH	Export to stream					
						Total BC	Total BC deep	Mg	K	Ca	Na
Export to stream	MTT	**1.00**									
	Log A	0.63*	**1.00**								
	M & L	−0.50	−0.20	**1.00**							
	pH	**0.87***	**0.80***	−0.52	**1.00**						
	Total BC	**0.77***	0.58*	−0.69*	**0.80***	**1.00**					
	Total BC Deep	**0.86***	0.69*	−0.58*	**0.87***	**0.97***	**1.00**				
	Mg	**0.78***	0.63*	−0.70*	**0.83***	**0.99***	**0.97***	**1.00**			
	K	**0.78***	0.58*	−0.57*	**0.73***	**0.95***	**0.95***	**0.93***	**1.00**		
	Ca	**0.83***	0.61*	−0.64*	**0.84***	**0.99***	**0.99***	**0.98***	**0.95***	**1.00**	
	Na	0.57*	0.42	**−0.79***	0.58*	**0.91***	**0.83***	**0.89***	**0.89***	**0.86***	**1.00**

be connected to processes not implemented in the model. As discussed above, several minerals with different weathering kinetics could contribute to the release of Mg and Ca to the groundwater, all of which are lumped together in the model. Although the model allows for some flexibility in the weathering kinetics, this may not be enough to fully capture the weathering dynamics of, for example, Ca, since there is a tendency to overestimate the weathering of Ca in small catchments and a similar tendency to underestimate its weathering in catchments with longer groundwater travel times. While it may be tempting to introduce a more complex weathering model to better capture this behaviour, the slight deviations could also be related mainly to minor problems in the predicted groundwater travel times. Hence, it is not obvious that a more complex weathering model would represent the real conditions more accurately, and there is always the risk of over-parameterisation. Other processes important for the weathering and transport of Mg and Ca, which seem more relevant to include in future models, are plant uptake, changes in the storage of exchangeable Mg and Ca due to acid precipitation (or recovery therefrom), and deposition changes. Harvesting and plant uptake changes can also cause changes in a watershed's base cation storage since trees and plants have significant contents of base cations (Gransee and Führs, 2013; Perakis et al., 2013). It was also recently reported that the Ca concentration in a stream in Krycklan has declined by 1.6 Ca μeq l^{-1} year^{-1} since the 1990s, probably due to decreasing levels of acid deposition (Laudon et al., 2021a). The model does not currently account for processes such as biological uptake and sorption, so it is not capable of handling these effects. However, it should be noted that this slow decline in Ca concentrations in stream water is weak compared to the gradients in the landscape that the model explains successfully. All these interconnected factors may affect Mg and Ca export on a shorter or longer time scale.

4.1.2. Potassium

The release of K was found to be strongly linked to the soil contact time (Fig. 6). This conclusion may seem surprising given that Erlandsson et al. (2016) reported that saturation with respect to K-feldspar can be observed within the upper metre of a soil profile in the area. However, the conclusion is strongly supported by the high K concentrations in streams with long groundwater travel times (Table 2). Apart from K-feldspar, significant amounts of K are also present in biotite. However, like K-feldspar, biotite is not particularly easily weathered. There could, however, be a non-stoichiometric release of K from the interlayers of biotite, which could explain why K concentrations increase continuously with the groundwater travel time despite the groundwater's apparent saturation with respect to the main K-bearing minerals (Erlandsson Lampa et al., 2020; Nyberg et al., 2001). A future groundwater geochemistry investigation could shed light on this issue and resolve some outstanding questions regarding the soil composition in the catchment (Lidman et al., 2019).

The model generally predicted annual K concentrations well but was less capable of capturing the observed seasonal variation for K than for Ca and Mg, especially in spring (Fig. 5). Presumably, it is the significant biological role of K that complicates the modelling of this element. The model does not currently account for any biological processes, and K should be the base cation most strongly affected by biological uptake and release. Studies on discharge dynamics have shown that K concentrations are less strongly connected to changes in stream flow than those of other base cations (i.e., the Q-C relationship is weaker for K than for other base cations) (Tripler et al., 2006). Leaves generally have higher concentrations of K than other base cations even though K is less strongly bound to the leaves' structural proteins and enzyme complexes than other base cations (Campo et al., 2000; Moslehi et al., 2019). The cycling of K into plants can reduce its available soil pool relative to that of Mg and Ca (Fig. 6) even when the supply (including that derived from plant matter) is ample (Frank and Stuanes, 2003). For example, the K concentration in spruce needles from C2 was found to be 12 mg g^{-1}, compared to 1.0 mg g^{-1} for Mg and 0.94 mg g^{-1} for Ca

(Lidman et al., 2017). A comparison of these values to the concentrations of the base cations in soil water and groundwater strongly suggests that the high mobility and leachability of K in dead and living plants (Salmon et al., 2001; Vitousek, 2004) causes leaf litter and plant uptake to have stronger seasonal impacts on concentrations of K than on those of other base cations (Tripler et al., 2006). For example, the impact of leaf litter from the previous autumn on the infiltration of snowmelt could explain why the model underestimated K concentrations in early spring (Fig. 5), while the somewhat overestimated concentrations in summer could be linked to the non-inclusion of plant uptake in the model.

4.1.3. Sodium

Sodium is one of the major cations in soils and practically all types of water. However, unlike K, Mg, and Ca, it is not considered a nutrient for most plants (Akselsson et al., 2019; Moslehi et al., 2019). Field observations in Krycklan have shown a rapid increase in the Na concentration after precipitation events in shallower soils. However, these increases are followed by sharp declines in the weathering rate in deeper groundwater. These observations are attributed to the groundwater reaching equilibrium with plagioclase, the only major Na-bearing mineral in these soils (Erlandsson Lampa et al., 2020). Smaller amounts of Na are probably also present in K-feldspar, but since the groundwater reaches equilibrium also with this mineral relatively rapidly, it probably does not contribute with much Na in deeper soils. This reduction in weathering rates is well reflected in the Na model by the high value of the b constant and the relatively high value of R_{max}, compared to the other base cations. Although the model could not capture all intra-annual variations, the correlation to observations was strong on both annual and seasonal time scales (Fig. 5). These results suggest that catchment export of Na to streams is not primarily correlated with MTT but rather with the presence of landscape features such as mires and lakes that dilute its concentration.

4.2. Catchment export of base cations and catchment characteristics

The export of base cations (especially Mg, K, and Ca) to streams within sub-catchments was closely linked to MTT (Table 2). Studies on stable water isotopes have indicated that the MTT is linked to the areal proportion of soils with low conductivity such as silty sediments (Jutebring Sterte et al., 2021a). Additionally, the chemical composition of the till and the sorted sediment soils in Krycklan was shown to be relatively uniform (Lidman et al., 2016). Despite this, the possibility that differences in the grain size distribution and the mineralogy of the finer soil fraction could affect the weathering rates cannot be excluded. However, the fact that a single weathering model could be applied to the whole catchment without accounting for potential differences in weathering rates between different soil types strongly suggests that MTT is the main factor responsible for the variation in base cation concentrations throughout the landscape. Unlike the other base cations, concentrations of Na were most strongly linked to the areal proportion of lakes and mires within sub-catchments (Table 2). In the streams, the dilution of water from the mires was more prominent for Na, probably because its weathering rate decreased most rapidly with soil depth (Fig. 6). Therefore, only a small portion of the total stream Na came from deep-soil weathering. Unlike the other base cations, the sharp weathering decline also caused the Na concentrations to be uncorrelated with changes in pH.

The proportion of deep-soil weathering, which contributed primarily to the stream concentrations of Mg and Ca, was also connected to the MTT (Table 2). It has been suggested that uncertainties about the weathering zone depth may be partly responsible for the some of the differences in published estimates of weathering rates in the same area (Futter et al., 2012; Whitfield et al., 2006), which can be substantial when comparing estimates obtained using different methods (Akselsson et al., 2019; Klaminder et al., 2011b). It has therefore been

suggested that multiple independent methods should be used when assessing weathering rates. Our results indicate that approximately 45% of the total base cation mass originates from sources well below the shallow soil (>2.5 m, Fig. 6). A limitation of our model's setup is that we cannot distinguish the importance of shallower weathering sources because shallow and deep weathering are only differentiated on the basis of the depth of the first saturated calculation layer, which is 2.5 m. A shallower deep-soil definition would have increased the contribution from "deep soils" even further. Our results thus suggest that substantial weathering occurs below the 0.5-1 m soil profiles that are considered in many common process-based weathering models (Akselsson et al., 2006; Akselsson and Belyazid, 2018; Phelan et al., 2014; Wallman et al., 2005).

While weathering below the root zone does not release nutrients accessible to forests (except in discharge areas), weathering is one of the most important acid-neutralising processes in the landscape and strongly affects the water quality and pH of downstream recipients such as streams and lakes (Larssen and Carmichael, 2000; Watmough et al., 2014). The correlation between base cation concentrations and pH directly illustrates the importance of weathering for stream water quality (Table 2). Therefore, even if deep weathering cannot supply the forests with nutrients, it can still be important for increasing the acid-neutralising capacity (ANC) of such groundwater recipients. Acidification of streams, lakes, and oceans is currently a sensitive issue in several countries (Broadmeadow et al., 2019; Geller and Schultze, 2009; Moiseenko et al., 2018). For example, one environmental goal presented by United Nations' 2030 Agenda for Sustainable Development is to address and minimise the impact of ocean acidification (Long, 2019). In Sweden, one of the environmental goals is to reduce anthropogenic acidification of streams and lakes (Naturvårdsverket, 2020). More specifically, the goal states that land use should not contribute to acidification. As acid precipitation has declined, the effects of forestry and other types of land use have become increasingly important. For example, the demand for renewable energy sources has led to increased terrestrial biomass extraction (Lamers et al., 2013). Therefore, information on the effects of deeper weathering on stream water quality will have direct practical implications for the sustainable management of boreal forests.

When forests take up base cations, they usually exchange them for protons, which leads to acidification of the soil water. This biological acidification is only temporary in natural forests, as base cations are returned when trees decompose. However, when biomass is harvested, the acidification becomes permanent (Moldan et al., 2017; Zhu et al., 2016). The maximum amount of biomass that can be removed from an area without soil acidification due to leaching has been defined as the *critical harvesting of biomass* (Akselsson and Belyazid, 2018). An analysis of Swedish soils using a shallow-soil weathering model indicated that stem harvesting may have caused the critical harvesting level to have been reached or even exceeded in some places, especially in southern Sweden (Akselsson et al., 2018), with several areas exceeding the critical outtake by 0.02-0.04 eq m^{-2} year^{-1} or more. However, our results suggest that deep sources may provide significant additional ANC, which was acknowledged but not accounted for by Akselsson et al. (2018). According to our calculations, deep base cation sources can increase the ANC by about 45% on average (Fig. 6). The additional weathering could reduce the number of acid-sensitive areas. However, our study also suggests that the contribution of deep weathering depends on catchment characteristics and varies considerably throughout the landscape. For example, streams draining catchments with short travel times (e.g., till-dominated areas) exported less base cations from deep-soil sources, making them more sensitive to acidification caused by harvesting (e.g., C2, Fig. 6).

Understanding the role of weathering and the evolution of groundwater chemistry in the landscape is also important for many other applications, such as assessing the transport and accumulation of various contaminants in the soils. Weathering-related parameters such as pH

and the concentrations of weathering-derived solutes can profoundly affect the speciation and mobility of many elements and compounds. One concrete example is the long-term safety of spent nuclear fuel repositories, which are typically located deep in the bedrock. The engineered barrier systems may be adversely affected by infiltration of dilute groundwater (SKB, 2011). However, while a prolonged period with a recharge of meteoric water could compromise repository integrity, the buffering capacity of the soil could also counteract the penetration of dilute water into the bedrock. Assessments of the buffering potential of soils based on a deep understanding and quantitative description of weathering processes are thus essential in hydrogeological applications such as site-descriptive modelling of potential repository sites (Selroos and Follin, 2014b) and safety assessments of such repositories (Selroos and Follin, 2014a).

In summary, our results imply that different methods should be considered when calculating base cation availability and its effect on terrestrial and aquatic ecosystems and water quality. Sustainable forestry is inseparably tied to the question of weathering because of its implications for management of forest soils and their nutrient balance as well as surface water quality and ecology. Conventional mass balance methods based on precipitation inputs and stream discharge outputs may overestimate the buffering potential and nutrient supply in shallow soils; for example, increasing deficiency of weathering-derived nutrients such as P, K, and Ca has been reported in coniferous forests (Quesnel and Côté, 2009). Meanwhile, predictive methods focusing on the shallow soil may underestimate the base cation content and buffering potential of water discharging into streams and lakes when applied to areas where deep soils are present and hydrologically active. The approach presented here circumvents these shortcomings and could thus help improve the prediction of base cation availability across catchments.

5. Conclusions and recommendations

This study aimed to investigate the dependencies of weathering rates of base cations on a catchment's hydrological functioning. The effects of catchment heterogeneity and scale on site hydrology and solute transport are not well understood but are nevertheless important for predicting and assessing water quality and the resilience of terrestrial and aquatic ecosystems. Although not all daily concentration variations were fully captured, the weathering model presented here successfully captured annual and seasonal variations in base cation concentrations and their general Q-C relationships in 14 sub-catchments with different landscapes, and explained most of the spatial differences observed within the studied catchment's stream network. The results obtained suggest that hydrological factors such as the mineral soil contact time strongly affect weathering and water quality. The four studied solutes responded in different ways to different catchment characteristics. Catchment export of Mg, K, and Ca was strongly correlated with MTT and deep-soil weathering, while Na export was more strongly correlated with the proportion of mires and lakes. The divergent behaviour of Na was linked to the rapid decrease in its weathering rates with increasing soil depth. The results presented here suggest that a significant fraction of catchment export can originate from deep-soil sources. When deep soils are present, methods focusing on the shallow soil might underestimate solute export, while mass balance methods might overestimate solutes accessible by plants. These results may have implications for climate and ecosystem studies, and the method used here could be a valuable tool for investigating weathering at different sites and scales that is complementary to existing methods. As such, it provides a robust foundation for future work on modelling weathering and solute transport. In future, the approach could be extended by including biochemical processes such as biological uptake and soil sorption, which would enable better prediction of changes in the concentrations of K and other more reactive solutes.

Data and code availability

Chemistry, environmental, and GIS data are available from Svartberget's open database, created in tandem with the Hydrological Research at Krycklan Catchment Study (Krycklan Database, 2013). The software and licence for Mike SHE and Mike 11 are available online (DHI, 2021). The Krycklan hydrological flow and weathering setup and input files can be acquired from the open database Safe Deposit (Jutebring Sterte et al., 2021b). Additionally, all sub-catchment results regarding flow and concentrations can be acquired from the open database Safe Deposit (Jutebring Sterte et al., 2021c).

CRediT authorship contribution statement

Elin Jutebring Sterte, Fredrik Lidman and Hjalmar Laudon were responsible for designing, conceptualising, and evaluating results in collaboration with the other co-authors. Elin and Emma Lindborg were responsible for the hydrological flow model setup, and Elin and Nicola Balbarini were responsible for the weathering model setup. Elin conducted the preparation of figures. She also led the writing of the paper with contributions from all co-authors.

Declaration of competing interest

The authors declare that they have no conflict of interest.

Acknowledgments

Supplementary data

Supplementary data to this article can be found online at https://doi.org/10.1016/j.scitotenv.2021.149101.

References

Abbott, B.W., Baranov, V., Mendoza-Lera, C., Nikolakopoulou, M., Harjung, A., Kolbe, T., Balasubramanian, M.N., Vaessen, T.N., Ciocca, F., Campeau, A., Wallin, M.B., Romeijn, P., Antonelli, M., Gonçalves, J., Datry, T., Laverman, A.M., de Dreuzy, J.-R., Hannah, D.M., Krause, S., Oldham, C., Pinay, G., 2016. Using multi-tracer inference to move beyond single-catchment ecohydrology. Earth Sci. Rev. 160, 19–42. https://doi.org/10.1016/j.earscirev.2016.06.014.

Abbott, B.W., Moatar, F., Gauthier, O., Fovet, O., Antoine, V., Ragueneau, O., 2018. Trends and seasonality of river nutrients in agricultural catchments: 18years of weekly citizen science in France. Sci. Total Environ. 624, 845–858. https://doi.org/10.1016/j.scitotenv.2017.12.176.

Ackerer, J., Steefel, C., Liu, F., Bart, R., Safeeq, M., O'Geen, A., Hunsaker, C., Bales, R., 2020. Determining how critical zone structure constrains hydrogeochemical behavior of watersheds: learning from an elevation gradient in California's Sierra Nevada. Front. Water 2, 23. https://doi.org/10.3389/frwa.2020.00023.

Akselsson, C., Belyazid, S., 2018. Critical biomass harvesting – applying a new concept for Swedish forest soils. For. Ecol. Manag. 409, 67–73. https://doi.org/10.1016/j.foreco.2017.11.020.

Akselsson, C., Sverdrup, H.U., Holmqvist, J., 2006. Estimating weathering rates of Swedish forest soils in different scales, using the PROFILE model and affiliated databases. J. Sustain. For. 21 (2–3), 119–131. https://doi.org/10.1300/J091v21n02_08.

Akselsson, C., Belyazid, S., 2018. Critical biomass harvesting – applying a new concept for Swedish forest soils. For. Ecol. Manage. 409, 67–73. https://doi.org/10.1016/j.foreco.2017.11.020.

Akselsson, C., Belyazid, S., Stendahl, J., Finlay, R., Olsson, B.A., Erlandsson Lampa, M., Wallander, H., Gustafsson, J.P., Bishop, K., 2019. Weathering rates in Swedish forest soils. Biogeosciences 16 (22), 4429–4450. https://doi.org/10.5194/bg-16-4429-2019.

Ameli, A.A., Beven, K., Erlandsson, M., Creed, I.F., McDonnell, J.J., Bishop, K., 2017. Primary weathering rates, water transit times, and concentration-discharge relations: a theoretical analysis for the critical zone. Water Resour. Res. 53 (1), 942–960. https://doi.org/10.1002/2016WR019448.

Anderson, S.P., Dietrich, W.E., Torres, R., Montgomery, D.R., Loague, K., 1997. Concentration-discharge relationships in runoff from a steep, unchanneled catchment. Water Resour. Res. 33 (1), 211–225. https://doi.org/10.1029/96WR02715.

Asano, Y., Compton, J.E., Church, M.R., 2006. Hydrologic flowpaths influence inorganic and organic nutrient leaching in a forest soil. Biogeochemistry 81 (2), 191–204. https://doi.org/10.1007/s10533-006-9036-4.

Augustin, F., Houle, D., Gagnon, C., Courchesne, F., 2016. Evaluation of three methods for estimating the weathering rates of base cations in forested catchments. Catena 144, 1–10. https://doi.org/10.1016/j.catena.2016.04.022.

Benettin, P., Bailey, S.W., Campbell, J.L., Green, M.B., Rinaldo, A., Likens, G.E., McGuire, K.J., Botter, G., 2015. Linking water age and solute dynamics in streamflow at the Hubbard brook experimental Forest, NH, USA. Water Resour. Res. 51 (11), 9256–9272. https://doi.org/10.1002/2015WR017552.

Bishop, K., Seibert, J., Nyberg, L, Rodhe, A., 2011. Water storage in a till catchment. II: implications of transmissivity feedback for flow paths and turnover times. Hydrol. Process. 25 (25), 3950–3959. https://doi.org/10.1002/hyp.8355.

Blumstock, M., Tetzlaff, D., Malcolm, I.A., Nuetzmann, G., Soulsby, C., 2015. Baseflow dynamics: multi-tracer surveys to assess variable groundwater contributions to montane streams under low flows. J. Hydrol. 527, 1021–1033. https://doi.org/10.1016/j.jhydrol.2015.05.019.

Botter, G., Bertuzzo, E., Rinaldo, A., 2010. Transport in the hydrologic response: travel time distributions, soil moisture dynamics, and the old water paradox. Water Resour. Res. 46 (3). https://doi.org/10.1029/2009WR008371.

Bouraoui, F., Grizzetti, B., 2011. Long term change of nutrient concentrations of rivers discharging in European seas. Sci. Total Environ. 409 (23), 4899–4916. https://doi.org/10.1016/j.scitotenv.2011.08.015.

Bricker, O.~.P., Jones, B.~.F., Bowser, C.~.J., 2003. Mass-balance approach to interpreting weathering reactions in watershed systems. Treatise Geochem. 5, 605. https://doi.org/10.1016/B0-08-043751-6/05180-X.

Broadmeadow, S.B., Nisbet, T.R., Forster, J., 2019. Trends in surface water chemistry in afforested Welsh catchments recovering from acidification, 1991–2012. Environ. Pollut. 247, 27–38. https://doi.org/10.1016/j.envpol.2018.12.048.

Butts, M., Loinaz, M., Gottwein, P.B., Unnasch, R., Gross, D., 2012. Mike She-Ecolab—an integrated catchment-scale eco-hydrological modelling tool. XIX international conference on water recourses CMWR 2012 University of Illinois at Urbana-Champaign, June 17–22, 2012.

Campo, J., Maass, J.M., Jaramillo, V.J., Yrízar, A.M., 2000. Calcium, potassium, and magnesium cycling in a Mexican tropical dry forest ecosystem. Biogeochemistry 49 (1), 21–36. https://doi.org/10.1023/A:1006207319622.

Casetou-Gustafson, S., Akselsson, C., Hillier, S., Olsson, B.A., 2019. The importance of mineral determinations to PROFILE base cation weathering release rates: a case study. Biogeosciences 16 (9), 1903–1920. https://doi.org/10.5194/bg-16-1903-2019.

DHI, 2021. MIKE powered by DHI – MIKE software. [online] Available from: https://www.mikepoweredbydhi.com/. (Accessed 10 March 2021).

Drever, J.I., 1994. The effect of land plants on weathering rates of silicate minerals. Geochim. Cosmochim. Acta 58 (10), 2325–2332. https://doi.org/10.1016/0016-7037(94)90013-2.

Dwivedi, R., Meixner, T., McIntosh, J.C., Ferré, P.A.T., Eastoe, C.J., Niu, G.-Y., Minor, R.L., Barron-Gafford, G.A., Chorover, J., 2019. Hydrologic functioning of the deep critical zone and contributions to streamflow in a high-elevation catchment: testing of multiple conceptual models. Hydrol. Process. 33 (4), 476–494. https://doi.org/10.1002/hyp.13363.

Egli, M., Fitze, P., 2000. Formulation of pedologic mass balance based on immobile elements: a revision. Soil Sci. 165 (5). https://doi.org/10.1097/00010694-200005000-00008.

Erlandsson Lampa, M., Sverdrup, H.U., Bishop, K.H., Belyazid, S., Ameli, A., Köhler, S.J., 2020. Catchment export of base cations: improved mineral dissolution kinetics influence the role of water transit time. Soil 6 (1), 231–244. https://doi.org/10.5194/soil-6-231-2020.

Erlandsson, M., Oelkers, E.H., Bishop, K., Sverdrup, H., Belyazid, S., Ledesma, J.L.J., Köhler, S.J., 2016. Spatial and temporal variations of base cation release from chemical weathering on a hillslope scale. Chem. Geol. 441, 1–13. https://doi.org/10.1016/j.chemgeo.2016.08.008.

Frank, J., Stuanes, A.O., 2003. Short-term effects of liming and vitality fertilization on forest soil and nutrient leaching in a scots pine ecosystem in Norway. For. Ecol. Manag. 176 (1), 371–386. https://doi.org/10.1016/S0378-1127(02)00285-2.

Futter, M.N., Klaminder, J., Lucas, R.W., Laudon, H., Köhler, S.J., 2012. Uncertainty in silicate mineral weathering rate estimates: source partitioning and policy implications. Environ. Res. Lett. 7 (2), 024025. https://doi.org/10.1088/1748-9326/7/2/024025.

Gabet, E.J., Edelman, R., Langner, H., 2006. Hydrological controls on chemical weathering rates at the soil-bedrock interface. Geology 34 (12), 1065. https://doi.org/10.1130/G23085A.1.

Gbondo-Tugbawa, S.S., Driscoll, C.T., 2003. Factors controlling long-term changes in soil pools of exchangeable basic cations and stream acid neutralizing capacity in a northern hardwood forest ecosystem. Biogeochemistry 63 (2), 161–185. https://doi.org/10.1023/A:1023308525316.

Geller, W., Schultze, M., 2009. Acidification. In: Likens, G.E. (Ed.), Encyclopedia of Inland Waters. Academic Press, Oxford, pp. 1–12.

Goddéris, Y., François, L.M., Probst, A., Schott, J., Moncoulon, D., Labat, D., Viville, D., 2006. Modelling weathering processes at the catchment scale: the WITCH numerical model. Geochim. Cosmochim. Acta 70 (5), 1128–1147. https://doi.org/10.1016/j.gca.2005.11.018.

Godsey, S.E., Kirchner, J.W., Clow, D.W., 2009. Concentration–discharge relationships reflect chemostatic characteristics of US catchments. Hydrol. Process. 23 (13), 1844–1864. https://doi.org/10.1002/hyp.7315.

Gransee, A., Führs, H., 2013. Magnesium mobility in soils as a challenge for soil and plant analysis, magnesium fertilization and root uptake under adverse growth conditions. Plant Soil 368 (1), 5–21. https://doi.org/10.1007/s11104-012-1567-y.

Herndon, E.M., Dere, A.L., Sullivan, P.L., Norris, D., Reynolds, B., Brantley, S.L., 2015. Landscape heterogeneity drives contrasting concentration–discharge relationships in shale headwater catchments. Hydrol. Earth Syst. Sci. 19 (8), 3333–3347. https://doi.org/10.5194/hess-19-3333-2015.

Hessen, D.O., Andersen, T., Tominaga, K., Finstad, A.G., 2017. When soft waters becomes softer; drivers of critically low levels of Ca in Norwegian lakes. Limnol. Oceanogr. 62 (1), 289–298. https://doi.org/10.1002/lno.10394.

Hrachowitz, M., Benettin, P., van Breukelen, B.M., Fovet, O., Howden, N.J.K., Ruiz, L., van der Velde, Y., Wade, A., 2016. Transit times—the link between hydrology and water quality at the catchment scale. Wiley Interdiscip. Rev. Water 3 (5), 629–657. https://doi.org/10.1002/wat2.1155.

Iwald, J., Löfgren, S., Stendahl, J., Karltun, E., 2013. Acidifying effect of removal of tree stumps and logging residues as compared to atmospheric deposition. For. Ecol. Manag. 290, 49–58. https://doi.org/10.1016/j.foreco.2012.06.022.

Jeziorski, A., Yan, N.D., Paterson, A.M., DeSellas, A.M., Turner, M.A., Jeffries, D.S., Keller, B., Weeber, R.C., McNicol, D.K., Palmer, M.E., McIver, K., 2008. The widespread threat of calcium decline in fresh waters. Science (80-.) 322, 1374–1377. https://doi.org/10.1126/science.1164949.

Jobbágy, E.G., Jackson, R.B., 2001. The distribution of soil nutrients with depth: global patterns and the imprint of plants. Biogeochemistry 53 (1), 51–77. https://doi.org/10.1023/A:1010760720215.

Joki-Heiskala, P., Johansson, M., Holmberg, M., Mattsson, T., Forsius, M., Kortelainen, P., Hallin, L., 2003. Long-Term Base cation balances of Forest mineral soils in Finland. Water Air Soil Pollut. 150 (1), 255–273. https://doi.org/10.1023/A:1026139730651.

Jutebring Sterte, E., Johansson, E., Sjöberg, Y., Huseby Karlsen, R., Laudon, H., 2018. Groundwater-surface water interactions across scales in a boreal landscape investigated using a numerical modelling approach. J. Hydrol. 560, 184–201. https://doi.org/10.1016/J.JHYDROL.2018.03.011.

Jutebring Sterte, E., Sjöberg, Y., Lindborg, E., Lidman, F., Laudon, H., Huseby Karlsen, R., 2021b. Surface-ground water interaction: from watershed processes to hyporheic exchange: Mike SHE Model 2021 Weathering (Accessed 10 Jun 2021). [online] Available from: https://www.safedeposit.se/projects/166.

Jutebring Sterte, E., Sjöberg, Y., Lindborg, E., Lidman, F., Laudon, H., Huseby Karlsen, R., 2021c. Surface-ground water interaction: from watershed processes to hyporheic exchange: Mike SHE Model 2021 Weathering and Flow Results (Accessed 10 Jun 2021). [online] Available from: https://www.safedeposit.se/projects/166.

Jutebring Sterte, E., Lidman, F., Lindborg, E., Sjöberg, Y., Laudon, H., 2021a. How catchment characteristics influence hydrological pathways and travel times in a boreal landscape. Hydrol. Earth Syst. Sci. 25 (4), 2133–2158. https://doi.org/10.5194/hess-25-2133-2021.

Karlsen, R.H., Grabs, T., Bishop, K., Buffam, I., Laudon, H., Seibert, J., 2016. Landscape controls on spatiotemporal discharge variability in a boreal catchment. Water Resour. Res. 52 (8), 6541–6556. https://doi.org/10.1002/2016WR019186.

Kirchner, J.W., Neal, C., 2013. Universal fractal scaling in stream chemistry and its implications for solute transport and water quality trend detection. Proc. Natl. Acad. Sci. 110 (30), 12213–12218. https://doi.org/10.1073/pnas.1304328110.

Kirchner, J.W., Feng, X., Neal, C., 2000. Fractal stream chemistry and its implications for contaminant transport in catchments. Nature 403 (6769), 524–527. https://doi.org/10.1038/35000537.

Klaminder, J., Grip, H., Morth, C.-M., Laudon, H., 2011a. Carbon mineralization and pyrite oxidation in groundwater: importance for silicate weathering in boreal forest soils and stream base-flow chemistry. Appl. Geochem. 26 (3), 319–324. https://doi.org/10.1016/j.apgeochem.2010.12.005.

Klaminder, J., Lucas, R., Futter, M., Bishop, K., Köhler, S., Gustaf, E., Laudon, H., 2011b. Silicate mineral weathering rate estimates: are they precise enough to be useful when predicting the recovery of nutrient pools after harvesting? For. Ecol. Manag. 261, 1–9. https://doi.org/10.1016/j.foreco.2010.09.040.

Kolbe, T., Marçais, J., de Dreuzy, J.R., Labasque, T., Bishop, K., 2020. Lagged rejuvenation of groundwater indicates internal flow structures and hydrological connectivity. Hydrol. Process. 34 (10), 2176–2189. https://doi.org/10.1002/hyp.13753.

Konrad, M., Schlingmann, K.P., Gudermann, T., 2004. Insights into the molecular nature of magnesium homeostasis. Am. J. Physiol. Physiol. 286 (4), F599-F605. https://doi.org/10.1152/ajprenal.00312.2003.

Koseva, I., Watmough, S., Aherne, J., 2010. Estimating base cation weathering rates in Canadian forest soils using a simple texture-based model. Biogeochemistry 101, 183–196. https://doi.org/10.1007/s10533-010-9506-6.

Krycklan Database, 2013. Hydrological research at Krycklan Catchment Study. [online] Available from: https://www.slu.se/krycklan. (Accessed 15 April 2021).

Lamers, P., Thiffault, E., Paré, D., Junginger, M., 2013. Feedstock specific environmental risk levels related to biomass extraction for energy from boreal and temperate forests. Biomass Bioenergy 55, 212–226. https://doi.org/10.1016/j.biombioe.2013.02.002.

Landeweert, R., Hoffland, E., Finlay, R.D., Kuyper, T.W., van Breemen, N., 2001. Linking plants to rocks: ectomycorrhizal fungi mobilize nutrients from minerals. Trends Ecol. Evol. 16 (5), 248–254. https://doi.org/10.1016/S0169-5347(01)02122-X.

Larssen, T., Carmichael, G.R., 2000. Acid rain and acidification in China: the importance of base cation deposition. Environ. Pollut. 110 (1), 89–102. https://doi.org/10.1016/S0269-7491(99)00279-1.

Laudon, H., Sponseller, R.A., 2018. How landscape organization and scale shape catchment hydrology and biogeochemistry: insights from a long-term catchment study. Wiley Interdiscip. Rev. Water 5 (2), e1265. https://doi.org/10.1002/wat2.1265.

Laudon, H., Taberman, I., Ågren, A., Futter, M., Ottosson-Löfvenius, M., Bishop, K., 2013. The Krycklan catchment study - a flagship infrastructure for hydrology, biogeochemistry, and climate research in the boreal landscape. Water Resour. Res. 49 (10), 7154–7158. https://doi.org/10.1002/wrcr.20520.

Laudon, H., Sponseller, R.A., Bishop, K., 2021a. From legacy effects of acid deposition in boreal streams to future environmental threats. Environ. Res. Lett. 16 (1), 15007. https://doi.org/10.1088/1748-9326/abd064.

Laudon, H., Hasselquist, E.M., Peichl, M., Lindgren, K., Sponseller, R., Lidman, F., Kuglerová, L., Hasselquist, N.J., Bishop, K., Nilsson, M.B., Ågren, A.M., 2021b. Northern landscapes in transition: evidence, approach and ways forward using the Krycklan catchment study. Hydrol. Process. 35 (4), e14170. https://doi.org/10.1002/hyp.14170.

Lawlor, D.W., 2004. Rieview of Principles of Plant Nutrition. In: Mengel, K, Kirby, EA (Eds.), 5th edn. Kluwer Academic Publishers, Dordrecht 2001. £220. (hardback). 849 pp.

Lebedeva, M.I., Brantley, S.L., 2020. Relating the depth of the water table to the depth of weathering. Earth Surf. Process. Landforms 45 (9), 2167–2178. https://doi.org/10.1002/esp.4873.

Lidman, F., Peralta-Tapia, A., Vesterlund, A., Laudon, H., 2016. 234U/238U in a boreal stream network — relationship to hydrological events, groundwater and scale. Chem. Geol. 420, 240–250. https://doi.org/10.1016/j.chemgeo.2015.11.014.

Lidman, F., Boily, Å., Laudon, H., Köhler, S.J., 2017. From soil water to surface water - how the riparian zone controls element transport from a boreal forest to a stream. Biogeosciences 14 (12), 3001–3014. https://doi.org/10.5194/bg-14-3001-2017.

Lidman, F., Laudon, H., Taberman, I., Köhler, S., 2019. Eu anomalies in soils and soil water from a boreal hillslope transect – a tracer for Holocene lanthanide transport? Geochim. Cosmochim. Acta 267, 147–163. https://doi.org/10.1016/j.gca.2019.09.014.

Long, J., 2019. (Honors College Theses). The United Nations' 2030 Agenda for Sustainable Development and the Impact of the Accounting Industry, p. 260. https://digitalcommons.pace.edu/honorscollege_theses/260.

Maher, K., 2010. The dependence of chemical weathering rates on fluid residence time. Earth Planet. Sci. Lett. 294 (1), 101–110. https://doi.org/10.1016/j.epsl.2010.03.010.

Maher, K., Druhan, J., 2014. Relationships between the transit time of water and the fluxes of weathered elements through the critical zone. Procedia Earth Planet. Sci. 10, 16–22. https://doi.org/10.1016/j.proeps.2014.08.004.

Maher, K., Steefel, C.I., White, A.F., Stonestrom, D.A., 2009. The role of reaction affinity and secondary minerals in regulating chemical weathering rates at the Santa Cruz soil chronosequence, California. Geochim. Cosmochim. Acta 73 (10), 2804–2831. https://doi.org/10.1016/j.gca.2009.01.030.

McDonnell, J.J., McGuire, K., Aggarwal, P., Beven, K.J., Biondi, D., Destouni, G., Dunn, S., James, A., Kirchner, J., Kraft, P., Lyon, S., Maloszewski, P., Newman, B., Pfister, L., Rinaldo, A., Rodhe, A., Sayama, T., Seibert, J., Solomon, K., Soulsby, C., Stewart, M., Tetzlaff, D., Tobin, C., Troch, P., Weiler, M., Western, A., Wörman, A., Wrede, S., 2010. How old is streamwater? Open questions in catchment transit time conceptualization, modelling and analysis. Hydrol. Process. 24 (12), 1745–1754. https://doi.org/10.1002/hyp.7796.

McLean, E.O., 1976. Chemistry of soil aluminum. Commun. Soil Sci. Plant Anal. 7 (7), 619–636. https://doi.org/10.1080/00103627609366672.

Moiseenko, T.I., Dinu, M.I., Gashkina, N.A., Jones, V., Khoroshavin, V.Y., Kremleva, T.A., 2018. Present status of water chemistry and acidification under nonpoint sources of pollution across European Russia and West Siberia. Environ. Res. Lett. 13 (10). https://doi.org/10.1088/1748-9326/aae268.

Moldan, F., Stadmark, J., Fölster, J., Jutterström, S., Futter, M.N., Cosby, B.J., Wright, R.F., 2017. Consequences of intensive forest harvesting on the recovery of Swedish lakes from acidification and on critical load exceedances. Sci. Total Environ. 603–604, 562–569. https://doi.org/10.1016/j.scitotenv.2017.06.013.

Moon, S., Chamberlain, C.P., Hilley, G.E., 2014. New estimates of silicate weathering rates and their uncertainties in global rivers. Geochim. Cosmochim. Acta 134, 257–274. https://doi.org/10.1016/j.gca.2014.02.033.

Moslehi, M., Habashi, H., Khormali, F., Ahmadi, A., Brunner, I., Zimmermann, S., 2019. Base cation dynamics in rainfall, throughfall, litterflow and soil solution under oriental beech (Fagus orientalis Lipsky) trees in northern Iran. Ann. For. Sci. 76 (2), 55. https://doi.org/10.1007/s13595-019-0837-8.

Naturvårdsverket, 2020. Miljömålen, Stockholm. [online] Available from: https://www.naturvardsverket.se/Documents/publ-filer/6900/978-91-620-6919-3.pdf?pid=26466.

Nieminen, M., Sarkkola, S., Tolvanen, A., Tervahauta, A., Saarimaa, M., Sallantaus, T., 2020. Water quality management dilemma: increased nutrient, carbon, and heavy metal exports from forestry-drained peatlands restored for use as wetland buffer areas. For. Ecol. Manag. 465, 118089. https://doi.org/10.1016/j.foreco.2020.118089.

Nyberg, L., 1995. Water flow path interactions with soil hydraulic properties in till soil at Gårdsjön, Sweden. J. Hydrol. 170 (1), 255–275. https://doi.org/10.1016/0022-1694(94)02667-Z.

Nyberg, L., Stähli, M., Mellander, P., Bishop, K.H., 2001. Soil frost effects on soil water and runoff dynamics along a boreal forest transect: 1. field investigations. Hydrol. Process. 15 (6), 909–926. https://doi.org/10.1002/hyp.256.

Ouimet, R., 2008. Using compositional change within soil profiles for modelling base cation transport and chemical weathering. Geoderma 145 (3), 410–418. https://doi.org/10.1016/j.geoderma.2008.01.007.

Ouimet, R., Duchesne, L., 2005. Base cation mineral weathering and total release rates from soils in three calibrated forest watersheds on the Canadian boreal shield. Can. J. Soil Sci. 85 (2), 245–260. https://doi.org/10.4141/S04-061.

Partington, D., Brunner, P., Frei, S., Simmons, C.T., Werner, A.D., Therrien, R., Maier, H.R., Dandy, G.C., Fleckenstein, J.H., 2013. Interpreting streamflow generation mechanisms from integrated surface-subsurface flow models of a riparian wetland and catchment. Water Resour. Res. 49 (9), 5501–5519. https://doi.org/10.1002/wrcr.20405.

Perakis, S.S., Sinkhorn, E.R., Catricala, C.E., Bullen, T.D., Fitzpatrick, J.A., Hynicka, J.D., Cromack Jr., K., 2013. Forest calcium depletion and biotic retention along a soil nitrogen gradient. Ecol. Appl. 23 (8), 1947–1961. https://doi.org/10.1890/12-2204.1.

Phelan, J., Belyazid, S., Kurz, D., Guthrie, S., Cajka, J., Sverdrup, H., Waite, R., 2014. Estimation of Soil Base cation weathering rates with the PROFILE model to determine critical loads of acidity for forested ecosystems in Pennsylvania, USA: pilot application of a potential National Methodology. Water Air Soil Pollut. 225 (9), 2109. https://doi.org/10.1007/s11270-014-2109-4.

Powers, S.M., Johnson, R.A., Stanley, E.H., 2012. Nutrient retention and the problem of hydrologic disconnection in streams and wetlands. Ecosystems 15 (3), 435–449. https://doi.org/10.1007/s10021-012-9520-8.

Quesnel, P.-O., Côté, B., 2009. Prevalence of phosphorus, potassium, and calcium limitations in white spruce across Canada. J. Plant Nutr. 32 (8), 1290–1305. https://doi.org/10.1080/01904160903006002.

Richardson, J.B., Petrenko, C.L., Friedland, A.J., 2017. Base cations and micronutrients in forest soils along three clear-cut chronosequences in the northeastern United States. Nutr. Cycl. Agroecosyst. 109 (2), 161–179. https://doi.org/10.1007/s10705-017-9876-4.

Salmon, C.D., Walter, M.T., Hedin, L.O., Brown, M.G., 2001. Hydrological controls on chemical export from an undisturbed old-growth Chilean forest. J. Hydrol. 253 (1), 69–80. https://doi.org/10.1016/S0022-1694(01)00447-4.

Schott, J., Pokrovsky, O.S., Oelkers, E.H., 2009. The link between mineral dissolution/precipitation kinetics and solution chemistry. Rev. Mineral. Geochem. 70 (1), 207–258. https://doi.org/10.2138/rmg.2009.70.6.

Seibert, J., Grabs, T., Köhler, S., Laudon, H., Winterdahl, M., Bishop, K., 2009. Linking soil- and stream-water chemistry based on a riparian flow-concentration integration model. Hydrol. Earth Syst. Sci. 13 (12), 2287–2297. https://doi.org/10.5194/hess-13-2287-2009.

Selroos, J.O., Follin, S., 2014a. Overview of hydrogeological safety assessment modeling conducted for the proposed high-level nuclear waste repository site at Forsmark, Sweden. Hydrogeol. J. 22 (6), 1229–1232. https://doi.org/10.1007/s10040-014-1163-8.

Selroos, J.O., Follin, S., 2014b. Overview of hydrogeological site-descriptive modeling conducted for the proposed high-level nuclear waste repository site at Forsmark, Sweden. Hydrogeol. J. 22 (2), 295–298. https://doi.org/10.1007/s10040-013-1077-x.

Sharpley, A.N., 1991. Effect of soil pH on cation and anion solubility. Commun. Soil Sci. Plant Anal. 22 (9–10), 827–841. https://doi.org/10.1080/00103629109368457.

SKB, 2011. Long-Term Safety for the Final Repository for Spent Nuclear Fuel at Forsmark: Main Report of the SR-Site Project, Stockholm.

Stewart, B.W., Capo, R.C., Chadwick, O.A., 2001. Effects of rainfall on weathering rate, base cation provenance, and sr isotope composition of Hawaiian soils. Geochim. Cosmochim. Acta 65 (7), 1087–1099. https://doi.org/10.1016/S0016-7037(00)00614-1.

Stumm, W., Wollast, R., 1990. Coordination chemistry of weathering: kinetics of the surface-controlled dissolution of oxide minerals. Rev. Geophys. 28 (1), 53–69. https://doi.org/10.1029/RG028i001p00053.

Sverdrup, H., Warfvinge, P., Blake, L., Goulding, K., 1995. Modelling recent and historic soil data from the Rothamsted Experimental Station, UK using SAFE. Agric. Ecosyst. Environ. 53 (2), 161–177. https://doi.org/10.1016/0167-8809(94)00558-V.

Swedish Geological Survey, 2016. Soil depth to bedrock map available at: https://www.sgu.se/en/products/maps. (last access: 18 April 2016).

Tiwari, T., Buffam, I., Sponseller, R.A., Laudon, H., 2017. Inferring scale-dependent processes influencing stream water biogeochemistry from headwater to sea. Limnol. Oceanogr. https://doi.org/10.1002/lno.10738.

Torres, M.A., West, A.J., Clark, K.E., 2015. Geomorphic regime modulates hydrologic control of chemical weathering in the Andes-Amazon. Geochim. Cosmochim. Acta 166, 105–128. https://doi.org/10.1016/j.gca.2015.06.007.

Tripler, C.E., Kaushal, S.S., Likens, G.E., Todd Walter, M., 2006. Patterns in potassium dynamics in forest ecosystems. Ecol. Lett. 9 (4), 451–466. https://doi.org/10.1111/j.1461-0248.2006.00891.x.

Van Meter, K.J., Basu, N.B., 2017. Time lags in watershed-scale nutrient transport: an exploration of dominant controls. Environ. Res. Lett. 12 (8), 84017. https://doi.org/10.1088/1748-9326/aa7bf4.

Velbel, M.A., Price, J.R., 2007. Solute geochemical mass-balances and mineral weathering rates in small watersheds: methodology, recent advances, and future directions. Appl. Geochem. 22 (8), 1682–1700. https://doi.org/10.1016/j.apgeochem.2007.03.029.

Vitousek, P.M., 2004. Nutrient Cycling and Limitation: Hawai'i as a Model System. Princeton University Press, Princeton.

Wallman, P., Svensson, M.G.E., Sverdrup, H., Belyazid, S., 2005. ForSAFE—an integrated process-oriented forest model for long-term sustainability assessments. For. Ecol. Manag. 207 (1), 19–36. https://doi.org/10.1016/j.foreco.2004.10.016.

Watmough, S.A., Whitfield, C.J., Fenn, M.E., 2014. The importance of atmospheric base cation deposition for preventing soil acidification in the athabasca Oil Sands region of Canada. Sci. Total Environ. 493, 1–11. https://doi.org/10.1016/j.scitotenv.2014.05.110.

Weill, S., Mazzia, A., Putti, M., Paniconi, C., 2011. Coupling water flow and solute transport into a physically-based surface–subsurface hydrological model. Adv. Water Resour. 34 (1), 128–136. https://doi.org/10.1016/j.advwatres.2010.10.001.

Weyhenmeyer, G.A., Hartmann, J., Hessen, D.O., Kopácek, J., Hejzlar, J., Jacquet, S., Hamilton, S.K., Verburg, P., Leach, T.H., Schmid, M., Flaim, G., Nõges, T., Nõges, P., Wentzky, V.C., Rogora, M., Rusak, J.A., Kosten, S., Paterson, A.M., Teubner, K., Higgins, S.N., Lawrence, G., Kangur, K., Kokorite, I., Cerasino, L., Funk, C., Harvey, R., Moatar, F., de Wit, H.A., Zechmeister, T., 2019. Widespread diminishing anthropogenic effects on calcium in freshwaters. Sci. Rep. 9 (1), 10450. https://doi.org/10.1038/s41598-019-46838-w.

Wilhelm, K., Rathsack, B., Bockheim, J., 2013. Effects of timber harvest intensity on macronutrient cycling in oak-dominated stands on sandy soils of northwest Wisconsin. For. Ecol. Manage. 291, 1–12. https://doi.org/10.1016/j.foreco.2012.10.047.

Whitfield, C.J., Watmough, S.A., 2012. A regional approach for mineral soil weathering estimation and critical load assessment in boreal Saskatchewan, Canada. Sci. Total Environ. 437, 165–172. https://doi.org/10.1016/j.scitotenv.2012.08.046.

Whitfield, C.J., Watmough, S.A., Aherne, J., Dillon, P.J., 2006. A comparison of weathering rates for acid-sensitive catchments in Nova Scotia, Canada and their impact on critical load calculations. Geoderma 136 (3), 899–911. https://doi.org/10.1016/j.geoderma.2006.06.004.

Xia, X.H., Wu, Q., Mou, X.L., Lai, Y.J., 2015. Potential impacts of climate change on the water quality of different water bodies. J. Environ. Inf. 25 (2), 85–98. https://doi.org/10.3808/jei.201400263.

Zanchi, G., 2016. Modelling Nutrient Transport From Forest Ecosystems to Surface Waters: The Model ForSAFE-2D. Lund University.

Zhu, Q., De Vries, W., Liu, X., Zeng, M., Hao, T., Du, E., Zhang, F., Shen, J., 2016. The contribution of atmospheric deposition and forest harvesting to forest soil acidification in China since 1980. Atmos. Environ. 146, 215–222. https://doi.org/10.1016/j.atmosenv.2016.04.023.